Development of a Brigatinib degrader (SIAIS117) as a potential treatment for ALK positive cancer resistance

Ning Sun, Chaowei Ren, Ying Kong, Hui Zhong, Jinju Chen, Yan Li, Jianshui Zhang, Yuedong Zhou, Xing Qiu, Haifan Lin, Xiaoling Song, Xiaobao Yang, Biao Jiang

PII: S0223-5234(20)30157-4

DOI: https://doi.org/10.1016/j.ejmech.2020.112190

Reference: EJMECH 112190

To appear in: *European Journal of Medicinal Chemistry*

Received Date: 17 December 2019

Revised Date: 24 February 2020

Accepted Date: 24 February 2020

Please cite this article as: N. Sun, C. Ren, Y. Kong, H. Zhong, J. Chen, Y. Li, J. Zhang, Y. Zhou, X. Qiu, H. Lin, X. Song, X. Yang, B. Jiang, Development of a Brigatinib degrader (SIAIS117) as a potential treatment for ALK positive cancer resistance, *European Journal of Medicinal Chemistry* (2020), doi: https://doi.org/10.1016/j.ejmech.2020.112190.

Development of a Brigatinib Degrader (SIAIS117) as a Potential Treatment for ALK Positive Cancer Resistance

Ning Sun[§†], Chaowei Ren[§†], Ying Kong[#], Hui Zhong[§▽], Jinju Chen[#], Yan Li[#], Jianshui Zhang[#], Yuedong Zhou[#], Xing Qiu[‡], Haifan Lin[§£]*, Xiaoling Song[§]*, Xiaobao Yang[§]* and Biao Jiang[§‡]*

[§]Shanghai Institute for Advanced Immunochemical Studies, ShanghaiTech University, 393 Middle Huaxia Road, Shanghai 201210, China

[‡]CAS Key Laboratory of Synthetic Chemistry of Natural Substances, Shanghai Institute of Organic Chemistry, Chinese Academy of Sciences, 345 Lingling Road, Shanghai 200032, China

[▽]Changzhou University, Changzhou, Jiangsu, 213164, China.

[£]Yale Stem Cell Center, Yale University, New Haven, CT 06511, USA.

[#]Jing Medicine Technology (Shanghai), Ltd., Y building, 230 Haike Road, Shanghai 201210, China

[+]These authors contributed equally to this work.

Abstract

EML4-ALK and NPM-ALK fusion proteins possess constitutively activated ALK (anaplastic lymphoma kinase) activity, which in turn leads to the development of non-small cell lung cancer and anaplastic large-cell lymphomas (ALCLs). FDA-approved ALK inhibitor drugs cause significant cancer regression. However, drug resistance eventually occurs and it becomes a big obstacle in clinic. Novel proteolysis targeting chimera (PROTAC) technology platform provides a potential therapeutic strategy for drug resistance. Herein, we designed and synthesized a series of ALK PROTACs based on Brigatinib and VHL-1 conjunction, and screened SIAIS117 as the best degrader which not only blocked the growth of SR and H2228 cancer cell lines, but also degraded ALK protein. In addition, SIAIS117 also showed much better growth inhibition effect than Brigatinib on 293T cell line that exogenously expressed G1202R-resistant ALK proteins. Furthermore, it also degraded G1202R mutant ALK protein *in vitro*. At last, it has the potentially anti-proliferation ability of small cell lung cancer. Thus, we have successfully generated the degrader SIAIS117 that can potentially overcome resistance in cancer targeted therapy.

Key words: ALK, Brigatinib, degrader, VHL, PROTAC, NSCLC, ALCL, resistance

1. Introduction

ALK is a tyrosine kinase that was firstly found in anaplastic large cell lymphoma[1]. It forms fusion proteins with more than 20 different genes in cancer. ALK fusion proteins can constitutively activate the ALK signaling pathway, which renders ALK a strong cancer driver gene[2, 3]. In lung cancer, the EML4-ALK (Echinoderm microtubule-associated protein-like 4) gene fusion is the most common form of ALK fusion. Cell lines with such mutations, including H2228, are highly dependent on ALK kinase activity; blocking ALK kinase activity greatly inhibits cancer cell growth[4-6]. ALK fusions are also present in approximately 60% anaplastic large-cell lymphomas (ALCLs) patients, and the major form of fusion is NPM-ALK. Different forms of the ALK fusion have been reported as cancer oncogenes that transform normal cells to cancer cells. The first generation ALK inhibitor drug Crizotinib was approved for the treatment of ALK-positive NSCLC patients as a first-in-class drug; however, resistance to Crizotinib occurs after treatment. To overcome the resistance, the second generation (Ceritinib, Alectinib, and Brigatinib) and third generation (Lorlatinib) drugs have been approved to treat NSCLC patients carrying an ALK fusion gene[7-11] (Figure 1). Despite the initial response to the second line use of such inhibitors, the majority of these patients eventually developed new resistances to these drugs[3, 12-14]. Therefore, our group construct protein degradation technology platform and devote to discovery of novel small molecule degraders for overcoming the treatment obstacle.

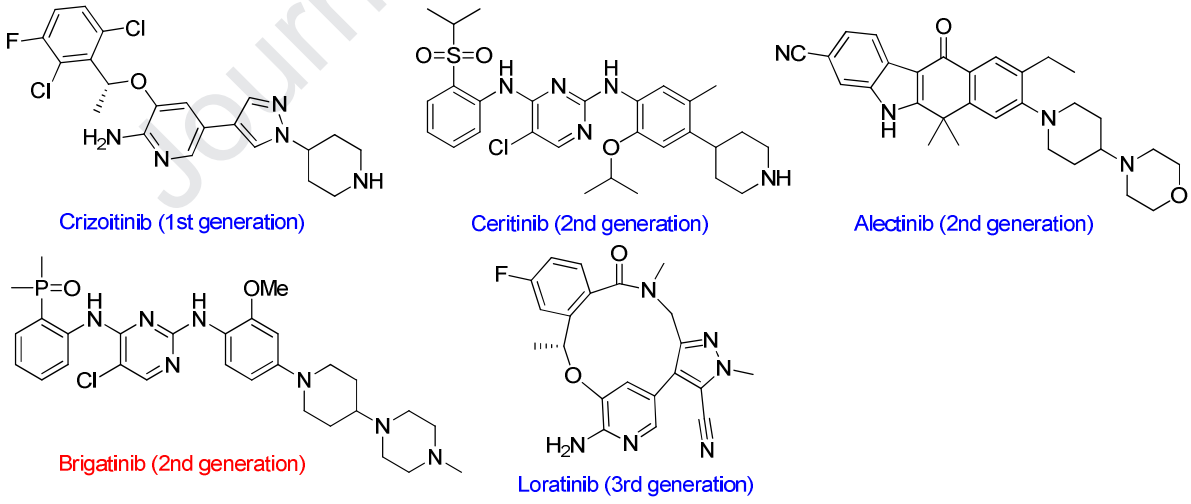

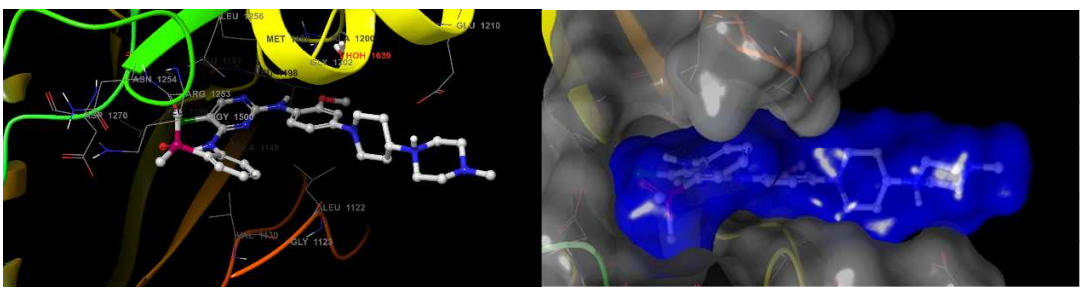

Figure 1 FDA-approved ALK drugs and the co-crystal structure of ALK with Brigatinib[a]

[a]The ligand interaction diagram is generated by Schrodinger.

PROTAC is a brand-new technology that has attracted considerable attention for its great potential as a promising cancer therapeutic strategy[15]. PROTAC molecules are bi-functional small molecules (Figure 2) that simultaneously bind to a target protein and an E3-ubiquitin ligase to establish a ternary complex. Because PROTAC molecules trigger ubiquitination and degradation of the target protein by the proteasome, they can degrade oncoproteins and theoretically can overcome drug resistance. This technology has been successfully applied to many target proteins, such as AR, ER, BET, FKBP-12, Bcr-Abl, PARP, BTK, EGFR, FLT-3,[16] TBK1, CDK4/6 and HER-2[17-32] used as the different E3 ligand including VHL-1, MDM2, CRBN and cIAP ligands (Figure 2).

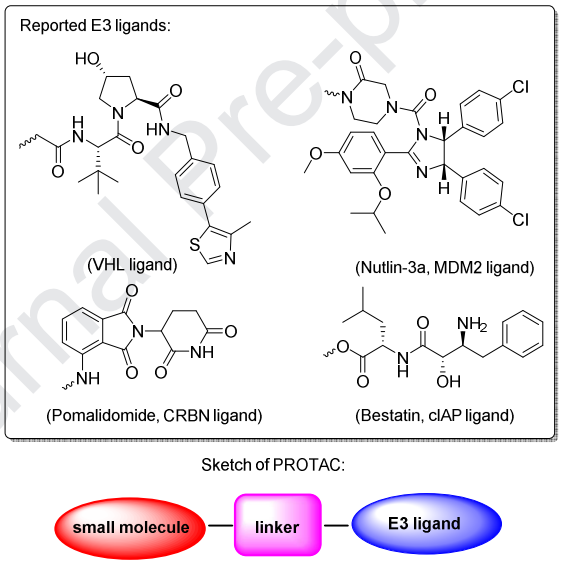

Figure 2. Reported E3 ligands and sketch of PROTAC

Recently, degraders of ALK also have been developed. Gray group reported an ALK degrader (**A)** (Figure 3) by linking ALK inhibitor Ceritinib to the CRBN E3 ligase ligand pomalidomide[24]. Jin and his colleagues also reported a potent Ceritinib-based ALK degrader[4] (**B**, **C)** (Figure 3). Hwang group reported ALK degrader (**D)** (Figure 3) by using Ceritinib to VHL-based PROTAC[19]. However, they all used Ceritinib as the ALK-binding moiety. To date, Brigatinib-based PROTAC targeting ALK has not been reported. There are many advantages of using Brigatinib over than ALK 2nd generation drugs. Brigatinib has more efficacy against most point mutant ALK than other second generation ALK drugs [33]. Brigatinib also induces intracranial response in patients, and was approved by FDA for treating patients with metastatic

non-small cell lung cancer[34]. Most importantly, patient received Brigatinib as their treatment showed higher overall response rate and had longer progression free survival comparing to other two 2nd ALK drugs[35, 36]. Based on these Brigatinib advantages, we selected Brigatinib as the PROTAC warhead. From co-crystal structure of ALK bound by Brigatinib (PDB ID: 6MX8), the solvent exposure piperidinyl part of Brigatinib is suitable for PROTAC design[37] (Figure 1, bottom), so we design a series of Brigatinib-PROTAC based on VHL E3 ligase.

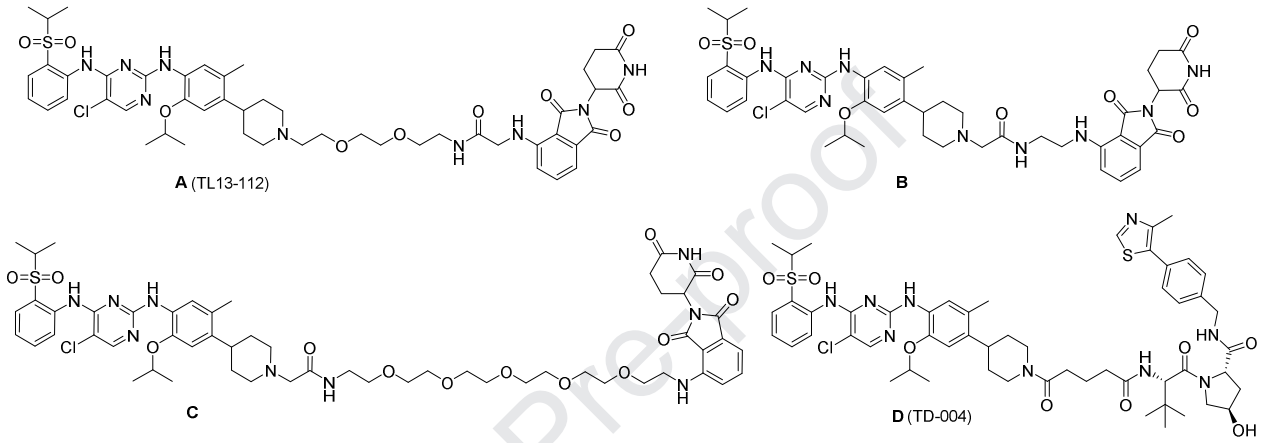

Figure 3. Reported potential ALK degraders

We successfully generated E3 VHL ligand and Brigatinib-based ALK degraders through two types of linkers. After exploration of the structure-activity relationships, we discovered that SIAIS117 degrades ALK protein level in a time- and dose-dependent manner. Firstly, this degrader not only inhibited the growth of ALK fusion positive ALCL cancer cell lines but also the growth of lung cancer cell line H2228 cells. Secondly, it effectively inhibited the growth of 293T cells that exogenously express resistant ALK fusion proteins and degraded G1202R mutant ALK protein in a dose-dependent manner. Thirdly, it inhibited the growth of small cell lung cancer cell lines. In summary, we successfully developed an ALK degrader and provides a promising tool to overcome ALK TKI resistance.

2. Result and discussion

2.1 Chemical Synthesis. Compounds **1, 2, 3, s-4, s-5, 4-38** were synthesized using the synthetic routes shown in Schemes 1−3. The preparation of compound **1-3** was started from 4-fluoro-2-methoxy-1-nitrobenzene [37]. Nucleophilic aromatic substitution reaction of the amino group under basic conditions provided intermediate **s-1**. Next, the NO_2 group on the phenyl ring were converted to NH_2 group under reduction reaction conditions, resulting in intermediate **s-2**, which was subsequently converted to **s-3** by microwave promoted Buchwald coupling. Boc

deprotection under acid conditions provided compound **1-3** (Scheme 1). Then, a linker library of VHL E3 ligase ligand VHL-1 were built (Scheme 2). The amino group of VHL-1 was reacted with various aliphatic acid to afford the linkers **s-4** and **s-5** (Scheme 2). Lastly, compound **1-3** condensed with various linkers to generate the corresponding ALK PROTACs **4-37** (Scheme 3). Furthermore, the negative control compound **38** (SIAIS117NC) could be synthesized from a similar route (Scheme 3).

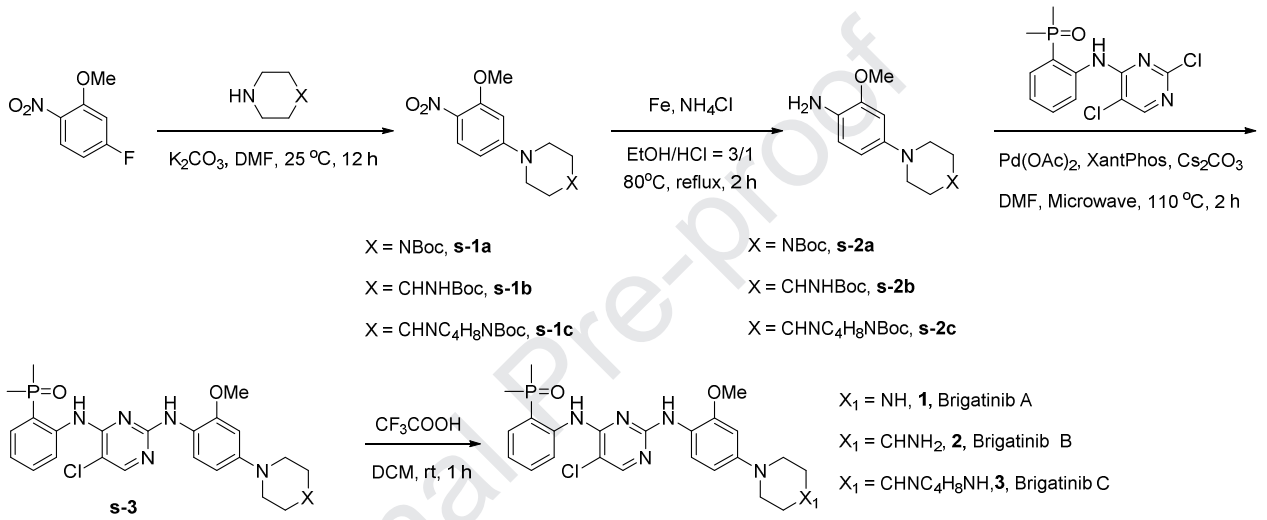

Scheme 1: Syntheses of Brigatinib analogue A、B、C

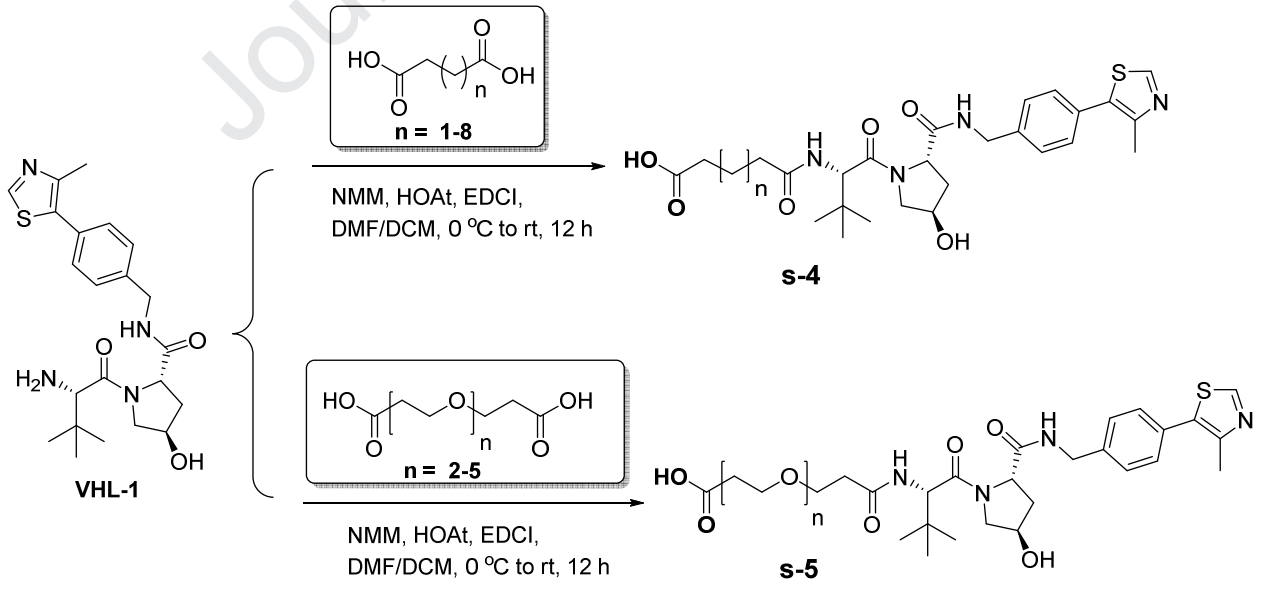

Scheme 2: Syntheses of VHL ligand based linkers

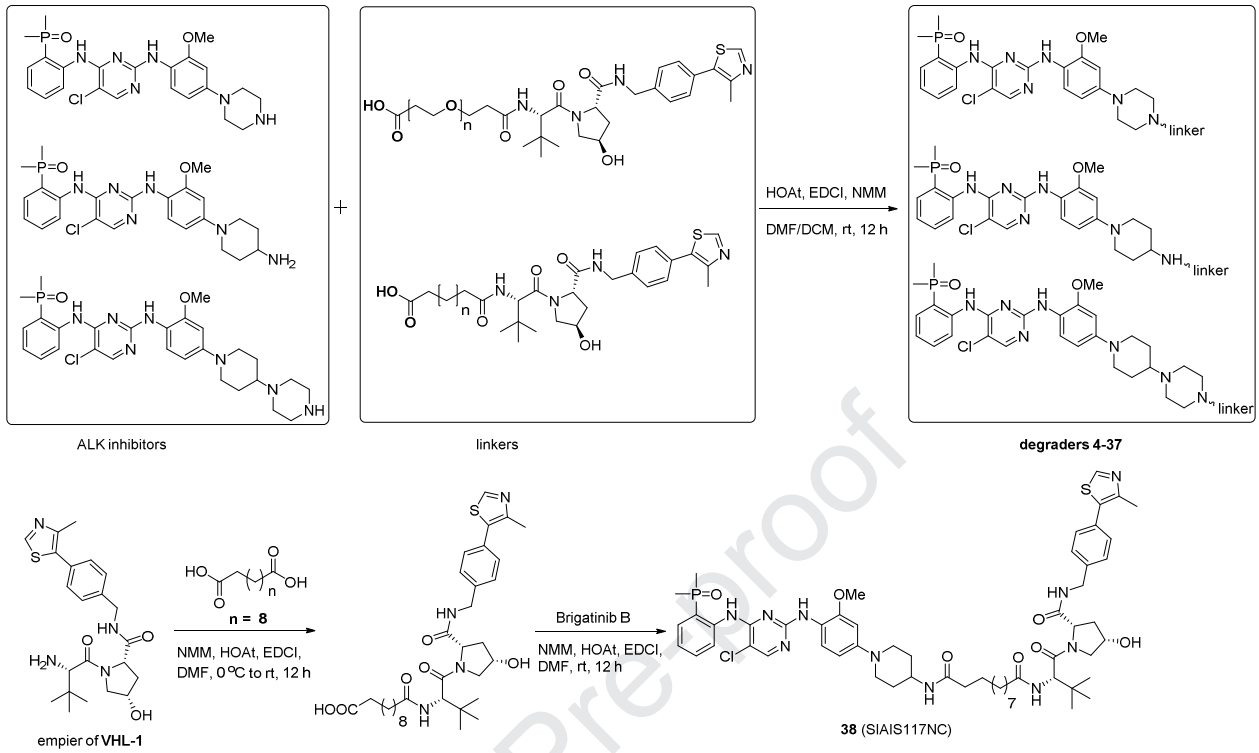

Scheme 3: Syntheses of ALK PROTACs

2.2 VHL-based ALK degraders inhibit the growth of ALK-fusion-positive cancer cells

Brigatinib, i*n vitro*, can inhibit the viability of cell lines carrying EML4-ALK fusion protein and 17 different ALK mutants conferring crizotinib resistance[37]. It has been approved by FDA for treating ALK-positive metastasized non-small cell lung cancer. Comparing to other two 2nd ALK drugs, Brigatinib showed better efficacies in improving overall response rate and progression free survival of crizotinib-refractory NSCLC patients[34-36, 38]. Therefore, we chose Brigatinib as the ALK binding moiety linking VHL ligands to generate PROTAC molecules.. ALCL SR cell line carrying NPM-ALK fusion gene is very sensitive to ALK inhibitors in our pre-test and was used in our screening (Table 1). Indeed, all three forms of Brigatinib can effectively inhibit the growth of SR cells, but there is no significant difference between Brigatinib analogs and the original drug (Table 1). In addition, Brigatinib and all three Brigatinib analogs did not degrade ALK proteins (Figure S2). These results indicated SR cell line is a good system to test our degraders.

compound	structure	SR IC_{50} (nM)[a]

Brigatinib	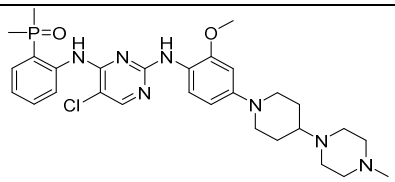	2.7±0.4
1 (Brigatinib A)	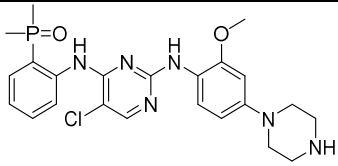	1.6±0.6
2 (Brigatinib B)	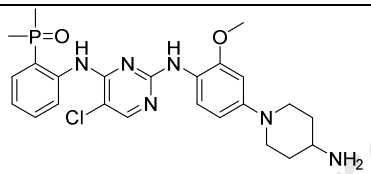	1.7±0.8
3 (Brigatinib C)	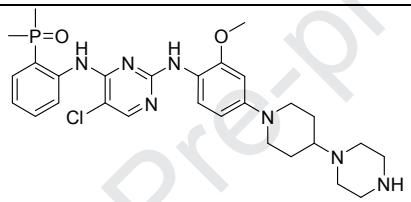	6.8±1.8

Table 1 Chemical Structures of three analogs of Brigatinib and their IC_{50} in SR cells. [a] IC_{50} values were obtained from three independent experiments.

The conjugation of three Brigatinib precursors with an alkyl VHL-1 library can efficiently generated PROTAC molecules (Figure 4A; see supporting information 1, 2 and 3). The changes of carbon-chain linkers interfered the growth inhibition effect on SR cell line. With increasing the length of the linker from C2 to C5, the growth inhibition ability became obviously weaker (as indicated as increase IC50 value), and then gradually increased from C6 to C8. Finally, Brigatinib B series showed the best growth inhibition effect with the same length linker compared with Brigatinib A and C series (Figure 4B). When the alkyl linkers length was increased to C9 to produce compound **18** (SIAIS117), the inhibitory activity of PROTAC compounds against SR growth was the strongest (IC_{50} = 1.7±1.0 nM). However, while using ethylenedioxy (-O-CH2-CH2-O-, abbreviated as PEG) linkers to generate three series Brigatinib degraders (Figure 4A), those degraders growth inhibition have sharply reduced in SR cell line (Figure 4C).

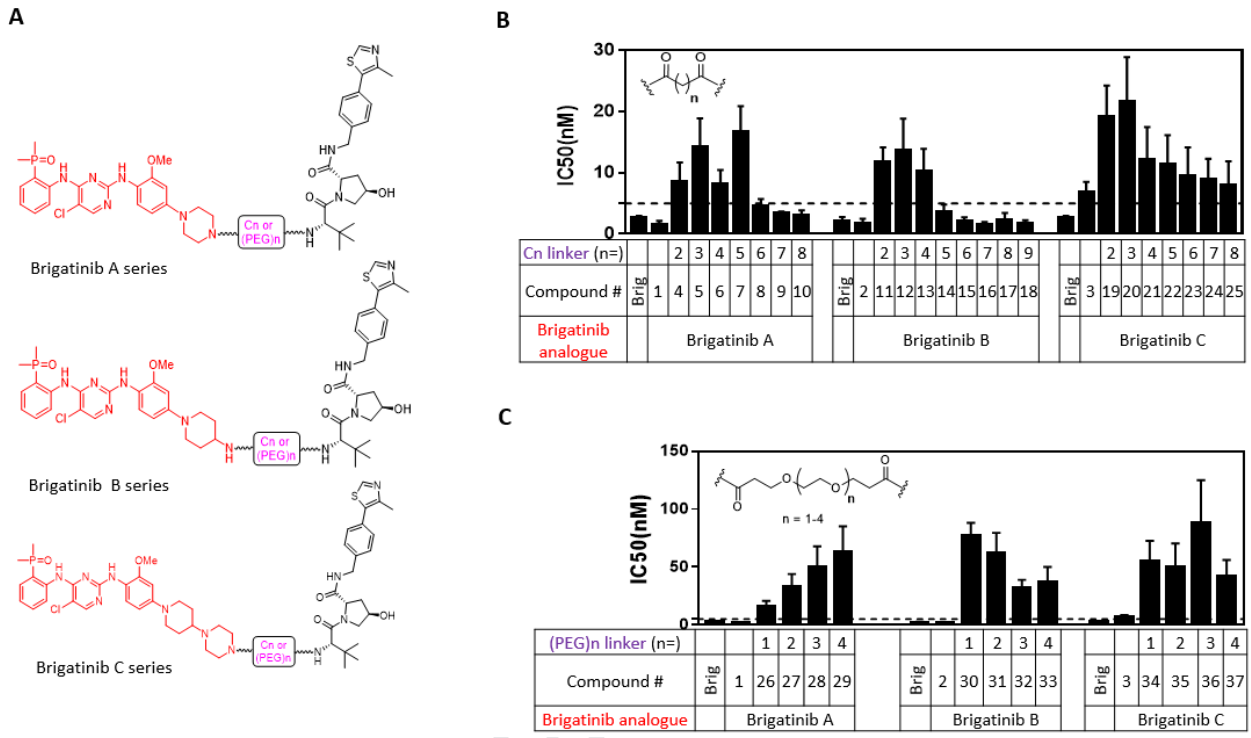

Figure 4: Optimization of linker type and length on the antiproliferative activity in SR. (A). Design and synthesis of Brigatinib A, B and C series degraders. (B). Study on the structure-activity relationship between carbon chain linker length and SR cell anti-proliferation ability, Cn stands for numbers for CH_2. (C). Study on the structure-activity relationship between PEG (-O-CH2-CH2-O-) linkers length and SR cell anti-proliferation ability.

2.3 ALK degraders effectively reduce ALK protein levels

Name	Series	carbon linker length	DC_{50} (nM) [a]
compound 8	Brigatinib A	6	>50
compound 9	Brigatinib A	7	15
compound 10	Brigatinib A	8	>50
compound 15	Brigatinib B	6	9.1
compound 16	Brigatinib B	7	20.9
compound 17	Brigatinib B	8	7.2
compound 23	Brigatinib C	6	11.4
compound 24	Brigatinib C	7	25.1
compound 25	Brigatinib C	8	7.5

compound 18 (SIAIS117)	Brigatinib B	9	7.0

Table 2 Optimization of linker type and length with regard to the degradative activity in SR. [a]DC50 are generated using gray value quantified by ImageJ.

ALK degraders can degrade ALK proteins at the concentration as low as 7.0 nM, and there was no obvious correlation between their degradation ability and cell growth inhibition was observed (Figure 4 and Table 2).Eventually, addition of PEG series of linker-based VHL compounds to Brigatinib resulted in loss of the growth inhibition effect on cancer cell lines. This effect did not change regardless whether A, B or C forms of Brigatinib analogue was used. When examined the ALK protein level, we found all these compounds cannot degrade ALK proteins. Thus, it indicates that PEG linkers are not tolerated with ALK fusion protein and VHL ligase.

2.4 ALK PROTAC degrades ALK proteins through the proteasome-mediated pathway

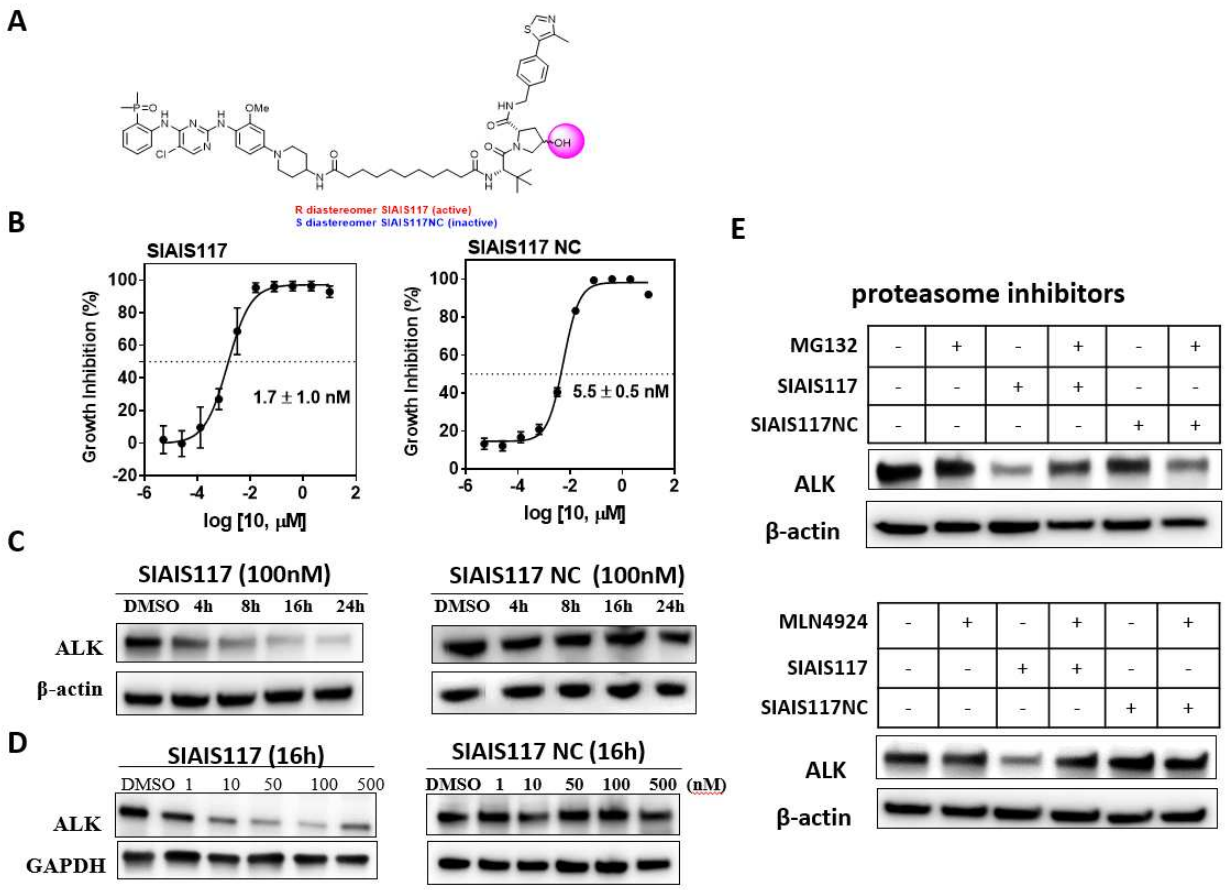

Figure 5 Mechanism of the ALK degradation induced by compound SIAIS117. (A). Structure of SIAIS117 and SIAIS117NC (Negative control). (B). The anti-proliferative activity of SIAIS117 and SIAIS117NC in SR. (C). Time course of SIAIS117 and SIAIS117NC (100 nM) in SR. (D). Concentration course SIAIS117NC in SR for 16 h. (E). SR cell line treated with proteasome inhibitor MG132 (5 μM) or SIAIS117, SIAIS117NC for 16 h. Data are representative of three independent experiments.

SIAIS117 degrades ALK in a time-dependent manner. To check how fast SIAIS117 will induce ALK protein degradation, we firstly treated SR cell line with 100 nM of compound SIAIS117, and then collected protein at indicated time points, and finally checked ALK protein levels (Figure 5C). After 4 hours treatment of SIAIS117, ALK protein started to be degraded, and 24 hours later, almost all ALK protein were degraded. To verify degrader works through proteasome-mediated pathway, we designed and synthesized a negative control compound **38** called as SIAIS117NC**,** an epimer of SIAIS117 (Figure 5A), which disturbing the binding at the E3 recruiting region. When the same amount of SIAIS117NC was used to treat SR cells, we did not detect any ALK protein degradation even after 24 hours (Figure 5C). We evaluated the degradation effect of Brigatinib in SR cell line, and found with varied time from 4 h to 24 hours and concentration from 30 nM to 300 uM, Brigatinib did not induce any reduction of ALK protein (Figure S4). We also found neither of the brigatinib isoforms degrade ALK proteins (Figure S2). Therefore, considering with a similar cellular permeability and kinase binding affinity for SIAIS117 and its epimer SIAIS117NC, a better growth inhibition effect on ALK mutant cancer was resulted from SIAIS117-induced ALK protein degradation (Fig. 5).

To further examine whether the degradation acted through the proteasome-mediated pathway, we also used proteasome inhibitors MG132 and MLN4924 to block proteasome function (Figure 5E). After pretreated cells with MG132 or MLN4924 for 4 hours, compound SIAIS117 or SIAIS117NC were used to treat SR cell line for 16 hours. Same as above, compound SIAIS117 degraded ALK protein in either case but negative control compound SIAIS117NC could not do so (Figure 5D and 5E). The degradation of ALK protein by SIAIS117 was rescued by pretreated cells with proteasome inhibitor MG132, and ALK protein levels turned back to normal. The same effect was observed when using MLN4924. This experiment further indicated that ALK PROTAC-induced ALK protein degradation act through proteasome mediated pathway.

2.5 ALK degrader retains ALK phosphorylation inhibition capability and inhibits signaling downstream of ALK.

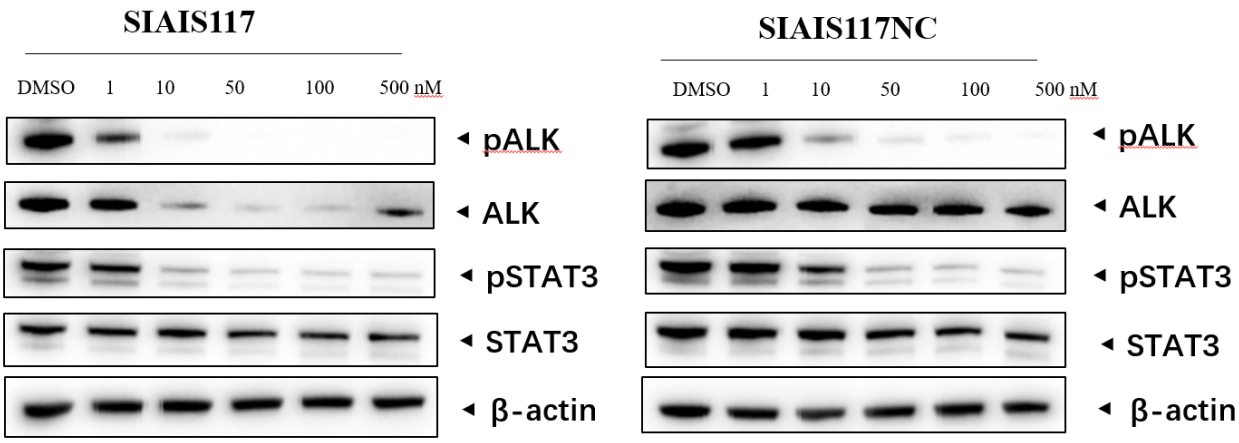

Figure 6 Compare SIAIS117 with negative control SIAIS117NC on degradative activity in SR. The degradative activity of SIAIS117 and SIAIS117NC in SR. Data are representative of three independent experiments.

We then studied the effects of SIAIS117 on the phosphorylation of ALK protein and signaling downstream of ALK. Compound SIAIS117 inhibited all of the phosphorylation of ALK at 10 nM (Figure 6). In comparison, it required approximately 50 nM of compound SIAIS117NC to achieve complete inhibition of the phosphorylation on ALK. We also checked ALK-mediated signaling after treatment with the two compounds. Compound SIAIS117 showed better inhibition of pSTAT3 than SIAIS117NC (Figure 6). Furthermore, proteomics data in SR cells (7280 proteins were identified) showed there was no other Brigatinib target kinase including EGFR mutations, IGF-1R, FLT3 and ROS1[39] degraded by SIAIS117 besides ALK fusion protein. In addition, there was also no significant change in the protein level of some kinases like Aurora A that were reported previously degraded by some ALK PROTAC molecules[24]. Among identified kinases in our proteomics data, UCK2 and GAK were also downregulated significantly. Conclusively, the selectivity of SIAIS117 is tending to be good in SR cell line (Figure S5, S6, Table S1).

2.6 ALK PROTAC compound SIAIS117 degrades ALK proteins and inhibits ALK phosphorylation in ALK mutant lung cancer cell lines.

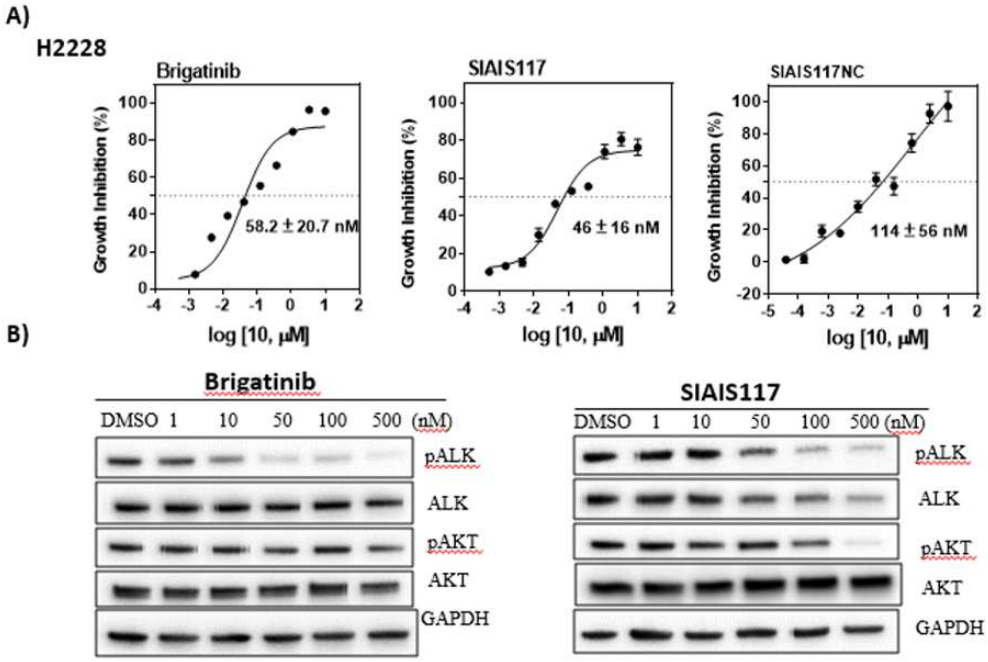

Figure 7 Degradative and inhibitory activities of compound SIAIS117 in NSCLC-H2228. (A). The anti-proliferative activity of Brigatinib, SIAIS117 and SIAIS117NC in H2228. (B). The degradative activity of Brigatinib and SIAIS117 in H2228. Data are representative of three independent experiments.

NSCLC cell line H2228 carries an EML4-ALK gene fusion and is sensitive to ALK inhibitors. After treating cells with drug for 72 h, living cells activities were evaluated by using CCK8 reagent (Figure 7A). Brigatinib inhibited H2228 cell growth with an IC_{50} around 58 nM. The designed degrader SIAIS117 kept the same potency level with Brigatinib. Compound SIAIS117 inhibited cell growth with an about two folds lower IC_{50} value (46 nM) comparing to SIAIS117NC (114 nM).

We next checked phosphorylation and degradation capability of the ALK protein after treating H2228 cell line with compound SIAIS117. While Brigatinib itself did not induce ALK protein degradation, compound SIAIS117 degraded ALK proteins at the concentration starting from 50 nM (Figure 7B).

2.7 ALK PROTAC compound SIAIS117 inhibited the growth of G1202R-mutant ALK cell line

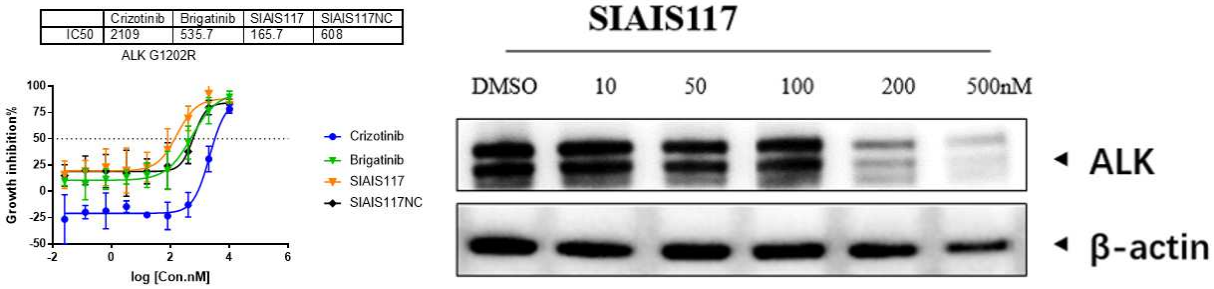

Figure 8 The ability of compound SIAIS117 in inhibiting the growth of G1202R-mutant ALK cell line and degrading G1202R-ALK protein. Left: growth inhibition assay; right: western blot. Data are representative of three independent experiments.

Point mutations of clinically Crizotinib-relevant resistance mutations include G1202R, G1269A, C1156Y, L1196M etc. G1202R mutation is a highly refractory mutation which is resistant to Crizotinib and all three 2nd generation ALK inhibitors including Ceritinib and Brigatinib[2]. To further investigate the ability of SIAIS117 to inhibit and degrade clinically relevant mutant isoforms, we exogenously expressed EML4-ALK with G1202R mutation in 293T cell line (Figure 8). SIAIS117 showed better growth inhibition than Brigatinib while SIAIS117NC had a similar growth inhibition compared to Brigatinib in 293T transduced with ALK G1202R. The IC_{50} values of Brigatinib or SIAIS117NC was approximately three times higher than that of SIAIS117 in this ALK mutant expressing cell lines (Figure 8). Due to the efficient inhibition effect (IC_{50} 146.4 nM) and degradation ability of SIAIS117 (DC_{50} < 200 nM) on ALK drug Crizotinib resistant cell lines, SIAIS117 provides a potential strategy to overcome G1202R-mediated drug resistance in ALK targeted therapy.

2.8 The anti-proliferation research against small cell lung cancer for ALK PROTAC compound SIAIS117

Transformation to small cell lung cancer is one of the resistant mechanisms in ALK- and EGFR-targeted therapy [40-43]. Small Cell Lung cancer (SCLC) is the most lethal lung cancer type. It progresses very fast, with cancer metastasis frequently already occurring before diagnosis. Given that SIAIS117 can effectively degrade ALK protein, we tested the effect of SIAIS117 in some SCLC cell lines although their proliferation did not rely on ALK protein expression. We found that SIAIS117 exerted the cell-killing effect of on small cell lung cancer cell lines (Figure 9). After treatment with SIAIS117 and Brigatinib, Brigatinib barely inhibited the growth of NCI-H69 cell line with an IC_{50} around 2.6 μM (Figure 9). However, SIAIS117 showed a lot better growth inhibition

effect on this cell line with an IC_{50} around 799 nM, which is achievable physiological range for many FDA approved drugs. To further exclude E3 ligand cell-killing effect, we picked up negative control E3 linker (**s-4h**) which had same length with SIAIS117, and found it did not inhibited the growth of NCI-H69 (IC_{50} > 40 μM). In another small cell lung cancer cell line NCI-H1688, and SIAIS117 showed a better anti-proliferation ability (IC_{50} = 259 nM) than Brigatinib (IC_{50} = 691 nM) and E3 linker s-4h (IC_{50} > 45 μM) (Figure 9). Similar rule was also observed for small cell lung cancer line NCI-H446. The reason why SIAIS117 inhibits growth of small cell lung cancer is under investigation.

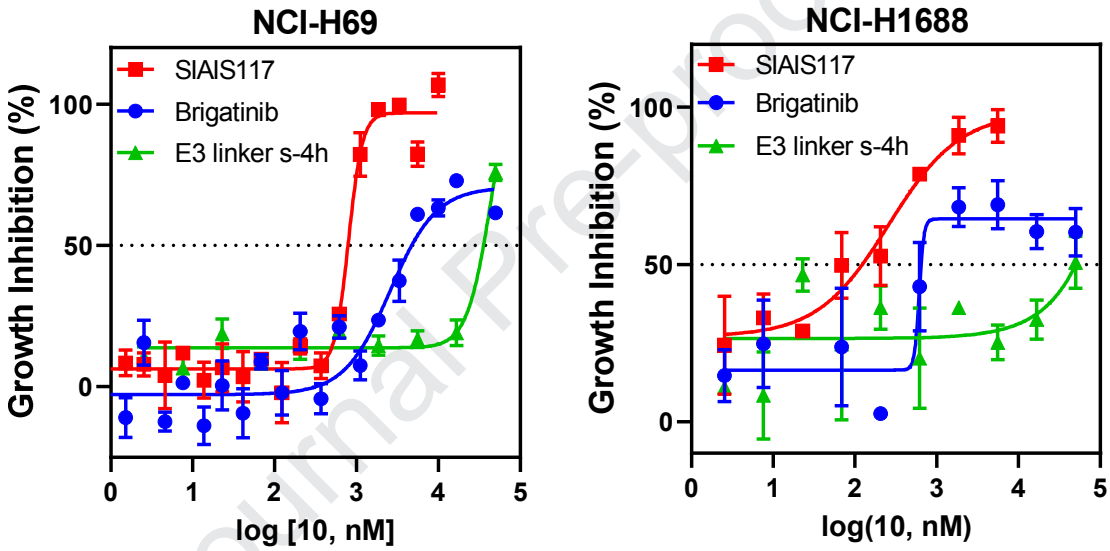

Figure 9 The ability of compound SIAIS117 to inhibit the growth of small cell lung cancer. Data are representative from at least three independent experiments. Two different small cell lung cancer cell lines were tested. Left: NCI-H69; right: NCI-H1688.

2.9 ALK PROTAC compound SIAIS117 maintained a longer degradative activity after drug removal

Next, we investigated the long-term degradation activity of SIAIS117. SIAIS117 was removed from medium after treating SR cells for 24 hours, and ALK protein levels were evaluated at 24h, 48h and 72hs after removal of SIAIS117. Results showed that SIAIS117 caused sustained degradation of ALK protein in SR cells (Figure 10). This result further illustrates that ALK degrader

maintained a longer cellular activity than that of ALK kinase inhibitor after short pulse of drug treatment. This provides a promising strategy to reduce side effect of Brigatinib drug and improving patients' quality of life in a more economical way.

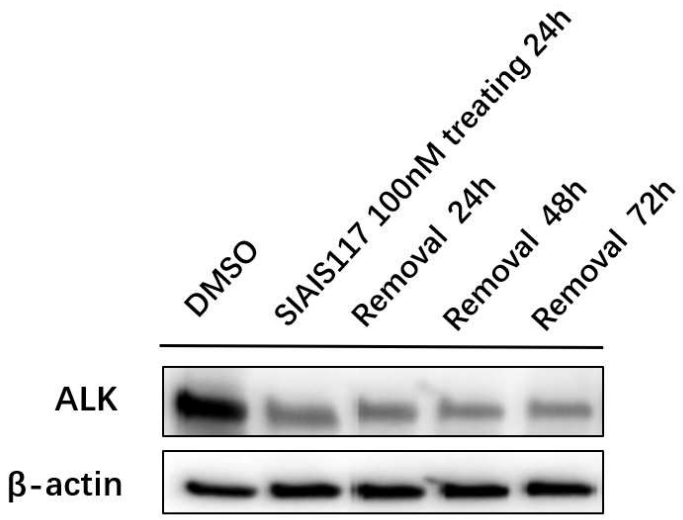

Figure 10 Sustained cellular degradative activity induced by **SIAIS117** after drug removal in SR cells. Cells was treated with 100 nM **SIAIS117** for 24 hours, following wash-out with drug free medium and then was incubated with drug-free medium. The ALK protein level was determined by western blot and normalized against β-actin.

3. Conclusions

We have successfully developed an ALK degrader, SIAIS117 that not only degrades but also inhibits the activities of oncogenic ALK protein in both non-small cell lung cancer H2228 cell and ALCL cell line SR cells. In addition, this compound displays a clear advantage in inhibiting the growth of cell line expressing G1202R-resistant ALK proteins and in degrading G1202R-resistant proteins. This is the novel reported ALK PROTAC molecule that can inhibit the growth of small cell lung cancer. Further studies will extend the application of ALK degrader in other ALK-positive cancer types.

4. EXPERIMENTAL SECTION

Chemistry. General Experiment and Information. Unless otherwise noted, all purchased reagents were used as received without further purification. *N*,*N*-diisopropylethylamine (DIPEA), *N*-methyl-2-pyrrolidinone (NMP), dichloromethane (DCM) and *N*,*N*-dimethylformamide (DMF)

were dried by a 4Å MS. Microwave reactions were performed with a CEM Discover single mode microwave reactor equipped with a 300W source under an atmosphere of dry argon. Flash chromatography was carried out on silica gel (200–300 mesh). ^{1}H NMR and ^{13}CNMR spectra were recorded on Bruker AVANCE III 500 MHZ (operating at 500 MHz for ^{1}H NMR, 126 MHz for ^{13}CNMR), chemical shift were reported in ppm relative to the residual d^{6}-DMSO (δ 2.50 ppm ^{1}H NMR) or CD_3OD (δ 3.31 ppm ^{1}H NMR). High Resolution Mass spectra were recorded on AB Triple 4600 spectrometer (QTOF) with acetonitrile and water as solvent. Preparative HPLC was performed on SHIMADZU LC-20AP series with UV detector set to 254 nm. The final compounds were all purified by C18 reverse phase preparative HPLC column with solvent A (0.5% HCl in H_2O) and solvent B (MeCN) as eluents. The purity of all the final compounds was confirmed to be >95% purity by HPLC (SHIMADZU).

General procedure for synthesis of compounds Brigatinib analogue A、B、C.

Typical procedure for the synthesis of (2-((5-chloro-2-((2-methoxy-4-(piperazin-1-yl)phenyl)amino)pyrimidin-4-yl)amino)phenyl) dimethylphosphine oxide 1 (Brigatinib A). To a solution of 5-fluoro-2-nitroanisole (7 g, 40.9 mmol) in DMF (60 mL) were added K_2CO_3 (8.4 g, 60.8 mmol) and tert-butyl piperazine-1-carboxylate (9.1 g, 48.9 mmol) at room temperature under air. After stirring at the same temperature overnight, then the reaction mixture was quenched with water, extracted with ethyl acetate, washed with brine and dried over anhydrous Na_2SO_4. The solvent was evaporated under the reduced pressure and the residue was purified by recrystallization (eluent: petroleum ether / ethyl acetate = 5:1) to afford **tert-butyl 4-(3-methoxy-4-nitrophenyl)piperazine-1-carboxylate s-1a** in 80% yield (11.1 g) as a yellow solid. ^{1}H NMR (500 MHz, DMSO) δ 7.89 (d, *J* = 9.3 Hz, 1H), 6.57 (d, *J* = 9.5 Hz, 1H), 6.52 (s, 1H), 3.90 (s, 3 H), 3.49-3.41 (m, 8H), 1.42 (s, 9H). HRMS (ESI) calcd for $C_{16}H_{24}N_3O_5^+$ $[M+H]^+$, 338.1710; found, 338.1705.

To a stirred solution of **s-1a** (10 g, 29.6 mmol) in EtOH (90 mL) and H_2O (30 mL) were added NH_4Cl (6.3 g, 118.6 mmol) and Fe powder (8.3 g, 148.2 mmol). Then the resulting mixture was refluxed at 80 ^{o}C for 2 h under an atmosphere of nitrogen. When the reaction was complete, the crude mixture was cooled down to room temperature, filtered by silica, after solvent evaporation, extracted with DCM (3 x 50 mL), the combined organic layer was washed with brine (20 mL), then dried over Na_2SO_4 and concentrated in vacuum to afford **tert-butyl**

4-(4-amino-3-methoxyphenyl)piperazine-1-carboxylate s-2a 7.7 g in 85% yield (11.1 g) as a gray solid. ^{1}H NMR (500 MHz, CD_3OD) δ 6.72 (d, *J* = 8.3 Hz, 1H), 6.63 (d, *J* = 2.2 Hz, 1H), 6.47 (d, *J* = 7.0 Hz, 1H), 3.86 (s, 3H), 3.57 (s, 4H), 2.99 (s, 4H), 1.50 (s, 9H). HRMS (ESI) calcd for $C_{16}H_{26}N_3O_3^+$ $[M+H]^+$, 308.1969; found, 308.1966.

To a solution of 2,5-dichloro-N-(2-(dimethylphosphoryl)phenyl)pyrimidin-4-amine (2 g, 6.3 mmol) in DMF (30 mL) were added **s-2a** (2.4 g, 7.8 mmol)，$Pd(OAc)_2$ (176 mg, 0.78 mmol)，Xantphos (810 mg, 1.4 mmol) and Cs_2CO_3(6.4 g, 19.6 mmol) in microwave tube, the solution was purged and refilled with nitrogen three times. Then the mixture was stirred at 110 ^{o}C for 2 h in the microwave. After the starting material was consumed, the reaction mixture was filtered through a pad of silica gel and most of the solvent of the filtrate was removed under the reduced pressure. Then the mixture was quenched with water, extracted with ethyl acetate, washed with water and brine, dried over anhydrous Na_2SO_4. The solvent was evaporated under the reduced pressure and the residue was purified by reverse phase ISCO (C18) to give the title compound **s-3a** as a brown solid.

To a solution of above compound **s-3a** (900 mg) in DCM (6 mL) were added CF_3COOH (2 mL) under air. The resulting solution was stirred at room temperature for 1 h. Then most of the solvent of the filtrate was removed under the reduced pressure, and adjusted the pH of the solution to 8-9 with saturated $NaHCO_3$ solution, extracted with DCM, washed with brine, dried over anhydrous Na_2SO_4. The solvent was evaporated under the reduced pressure and the residue was purified by reverse phase ISCO (C18) to afford **(2-((5-chloro-2-((2-methoxy-4-(piperazin-1-yl)phenyl)amino)pyrimidin-4-yl)amino)phenyl) dimethylphosphine oxide 1 (Brigatinib A)** as a yellow solid (701 mg, 23% yield over two steps). ^{1}H NMR (500 MHz, CD_3OD) δ 8.32 (dd, *J* = 8.2, 4.4 Hz, 1H), 8.04 (s, 1H), 7.70 (d, *J* = 8.7 Hz, 1H), 7.61 (dd, *J* = 14.1, 7.7 Hz, 1H), 7.52 (t, *J* = 7.9 Hz, 1H), 7.26 (t, *J* = 7.5, 1H), 6.67 (d, *J* = 2.5 Hz, 1H), 6.45 (dd, *J* = 8.8, 2.5 Hz, 1H), 3.86 (s, 3H), 3.24 - 3.17 (m, 4H), 3.17 - 3.11 (m, 4H), 1.83 (d, *J* = 13.5 Hz, 6H). HRMS (ESI) calcd for $C_{23}H_{29}ClN_6O_2P^+$ $[M+H]^+$, 487.1773; found, 487.1772.

(2-((2-((4-(4-aminopiperidin-1-yl)-2-methoxyphenyl)amino)-5-chloropyrimidin-4-yl)amino)phenyl)dimethylphosphine oxide (Brigatinib B, 2). (yellow solid, 330 mg, 33% yield over two steps) ^{1}H NMR (500 MHz, DMSO) *δ* 8.49 (s, 1H), 8.08 (s, 1H), 8.06 (s, 1H), 7.53 (ddd, *J* = 14.0,

7.7, 1.3 Hz, 1H), 7.38 – 7.32 (m, 2H), 7.10 (t, *J* = 7.1 Hz, 1H), 6.62 (d, *J* = 2.5 Hz, 1H), 6.46 (dd, *J* = 8.7, 2.5 Hz, 1H), 3.75 (s, 3H), 3.65 – 3.61 (m, 2H), 2.78 – 2.67 (m, 3H), 1.82 – 1.79 (m, 2H), 1.78 (s, 3H), 1.75 (s, 3H), 1.42 – 1.34 (m, 2H). HRMS (ESI) calcd for $C_{24}H_{31}ClN_6O_2P$ $[M+H]^+$: 501.1913, found 501.1905.

(2-((5-chloro-2-((2-methoxy-4-(4-(piperazin-1-yl)piperidin-1-yl)phenyl)amino)pyrimidin-4-yl)amino)phenyl)dimethylphosphine oxide (Brigatinib C, 3). (yellow solid, 350 mg, 37% yield over two steps). ^{1}H NMR (500 MHz, CD_3OD) δ 8.33 (dd, *J* = 8.2, 4.4 Hz, 1H), 8.03 (s, 1H), 7.69 – 7.64 (m, 1H), 7.61-7.60 (m, 1H), 7.51 (t, *J* = 7.9 Hz, 1H), 7.28-7.24 (m, 1H), 6.66 (d, *J* = 2.4 Hz, 1H), 6.45 (dd, *J* = 8.8, 2.5 Hz, 1H), 3.85 (s, 3H), 3.73 – 3.63 (m, 2H), 3.11 – 3.02 (m, 4H), 2.79 – 2.66 (m, 6H), 2.48-2.43 (m, 1H), 1.99 (d, *J* = 12.5 Hz, 2H), 1.84 (d, *J* = 13.5 Hz, 6H), 1.72 – 1.63 (m, 2H). HRMS (ESI) calcd for $C_{28}H_{38}ClN_7O_2P$ $[M+H]^+$: 570.2508, found 570.2506.

General procedure for synthesis of VHL linkers s-4, s-5

To a stirred solution of succinic acid (680 mg, 5.8 mmol) in DMF (10 mL) was added anhydrous DCM (150 mL). Then the mixture was cooled to 0 ^{o}C, NMM (1.16 g, 11.5 mmol), VHL-1 (1.0 g, 2.3 mmol), HOAT (63 mg, 0.46 mmol) and EDCI.HCl (530 mg, 2.8 mmol) were added sequentially. The solution was purged and refilled with nitrogen. The resulting mixture was stirred at room temperature for 12 h. The reaction mixture was quenched with water (1 mL). After concentration, the residue was purified reverse phase ISCO (C18) to afford the desired compound **s-4a**

(4-(((S)-1-((2S,4R)-4-hydroxy-2-((4-(4-methylthiazol-5-yl)benzyl)carbamoyl)pyrrolidin-1-yl)-3,3-dimethyl-1-oxobutan-2-yl)amino)-4-oxobutanoic acid) (s-4a) (0.82 g, 65% yield) as a white solid. ^{1}H NMR (500 MHz, $CDCl_3$) *δ* 11.88 (s, 1H), 8.85 (s, 1H), 7.69 (s, 1H), 7.37 – 7.29 (m, 4H), 6.09 (br, 1H), 4.67 – 4.54 (m, 3H), 4.49 (s, 1H), 4.29 (dd, *J* = 15.0, 5.0Hz, 1H), 4.05 (d, *J* = 11.3 Hz, 1H), 3.73 – 3.63 (m, 1H), 2.73 – 2.58 (m, 1H), 2.57 – 2.41 (m, 3H), 2.50 (s, 3H), 2.31 – 2.14 (m, 2H), 0.96 (s, 9H). HRMS (ESI) m/z: cal. $C_{26}H_{35}N_4O_6S^+$ $[M+H]^+$, 531.2272; found. 531.2280.

5-(((S)-1-((2S,4R)-4-hydroxy-2-((4-(4-methylthiazol-5-yl)benzyl)carbamoyl)pyrrolidin-1-yl)-3,3-dimethyl-1-oxobutan-2-yl)amino)-5-oxopentanoic acid (s-4b). (white solid, 0.85 g, 67%). ^{1}H NMR (500 MHz, $CDCl_3$) *δ* 9.08 (s, 1H), 8.10 (s, 1H), 7.38 – 7.29 (m, 4H), 4.72 – 4.64 (m, 3H), 4.52 (s, 1H), 4.25 (dd, *J* = 15.4, 5.0 Hz, 1H), 4.09 (d, *J* = 10.5 Hz, 1H), 3.73 (d, *J* = 10.0 Hz, 1H), 2.48 (s, 3H), 2.39 – 2.13 (m, 6H), 1.92 – 1.74 (m, 2H), 0.96 (s, 9H). HRMS (ESI) m/z: cal. $C_{27}H_{37}N_4O_6S^+$ $[M+H]^+$, 545.2428; found. 545.2436.

6-(((S)-1-((2S,4R)-4-hydroxy-2-((4-(4-methylthiazol-5-yl)benzyl)carbamoyl)pyrrolidin-1-yl)-3,3-dimethyl-1-oxobutan-2-yl)amino)-6-oxohexanoic acid (s-4c). (white solid, 0.79 g, 55%) ^{1}H NMR (500 MHz, $CDCl_3$) δ 8.99 (s, 1H), 7.66 (s, 1H), 7.39 – 7.33 (m, 4H), 7.30 (d, J = 7.5 Hz, 1H), 7.14 (br, 1H), 4.67 – 4.61 (m, 3H), 4.52 (s, 1H). 4.28 (dd, J = 15.4, 5.0 Hz, 1H), 4.09 (d, J = 11.4 Hz, 1H), 3.74 – 3.63 (m, 1H), 2.52 (s, 3H), 2.31 – 2.17 (m, 6H), 1.65 – 1.53 (m, 4H), 0.96 (s, 9H). HRMS (ESI) m/z: cal. $C_{28}H_{40}N_4O_6S^+$ $[M+H]^+$, 559.2585; found. 559.2590.

7-(((S)-1-((2S,4R)-4-hydroxy-2-((4-(4-methylthiazol-5-yl)benzyl)carbamoyl)pyrrolidin-1-yl)-3,3-dimethyl-1-oxobutan-2-yl)amino)-7-oxoheptanoic acid (s-4d). (white solid, 0.80 g, 57%) ^{1}H NMR (500 MHz, $CDCl_3$) δ 8.90 (s, 1H), 7.42 – 7.38 (m, 1H), 7.41 – 7.33 (m, 4H), 7.31 (d, J = 9.0 Hz, 1H), 6.50 (br, 1H), 4.79 – 4.46 (m, 3H), 4.55 (s, 1H), 4.28 (dd, J = 15.2, 5.1 Hz, 1H), 4.12 (d, J = 11.3 Hz, 1H), 3.72 – 3.63 (m, 1H), 2.51 (s, 3H), 2.38 – 2.33 (m, 1H), 2.28 – 2.21 (m, 4H), 2.18 – 2.12 (m, 1H), 1.62 – 1.51 (m, 4H), 1.33 – 1.26 (m, 4H), 0.96 (s, 9H). HRMS (ESI) m/z: cal. $C_{29}H_{41}N_4O_6S^+$ $[M+H]^+$, 573.2741; found. 573.2738.

8-(((S)-1-((2S,4R)-4-hydroxy-2-((4-(4-methylthiazol-5-yl)benzyl)carbamoyl)pyrrolidin-1-yl)-3,3-dimethyl-1-oxobutan-2-yl)amino)-8-oxooctanoic acid (s-4e). (white solid, 0.95 g, 68%) ^{1}H NMR (500 MHz, $CDCl_3$) δ 8.82 (s, 1H), 7.43 (t, J = 6.0 Hz, 1H), 7.36 – 7.34 (m, 4H), 6.98 (d, J = 8.5 Hz, 1H), 6.10 (br, 1H), 4.69 – 4.65 (m, 1H), 4.63 – 4.51 (m, 2H), 4.55 – 4.50 (m, 1H), 4.38 – 4.27 (m, 1H), 4.11 (d, J = 16.7 Hz, 1H), 3.72 – 3.62 (m, 1H), 2.51 (s, 3H), 2.39 – 2.13 (m, 6H), 1.58 – 1.54 (m, 4H), 1.33 – 1.21 (m, 4H), 0.95 (s, 9H). HRMS (ESI) m/z: cal. $C_{30}H_{43}N_4O_6S^+$ $[M+H]^+$, 587.2898; found. 587.2907.

9-(((S)-1-((2S,4R)-4-hydroxy-2-((4-(4-methylthiazol-5-yl)benzyl)carbamoyl)pyrrolidin-1-yl)-3,3-dimethyl-1-oxobutan-2-yl)amino)-9-oxononanoic acid (s-4f). (white solid, 0.92 g, 64%). ^{1}H NMR (500 MHz, $CDCl_3$) δ 8.82 (s, 1H), 7.35 (s, 4H), 7.00 (d, J = 10.0 Hz, 1H), 5.99 (br, 1H), 4.74 – 4.49 (m, 4H), 4.30 (dd, J = 15.2, 5.1 Hz, 1H), 4.13 (d, J = 11.3 Hz, 1H), 3.67 (dd, J = 11.5, 3.5 Hz, 1H), 2.51 (s, 3H), 2.42 – 2.36 (m, 1H), 2.28 (t, J = 7.5 Hz, 2H), 2.24 – 2.12 (m, 3H), 1.67 – 1.48 (m, 4H), 1.35 – 1.22 (m, 6H), 0.95 (s, 9H). HRMS (ESI) m/z: cal. $C_{31}H_{45}N_4O_6S^+$ $[M+H]^+$, 601.3054; found. 601.3060.

10-(((S)-1-((2S,4R)-4-hydroxy-2-((4-(4-methylthiazol-5-yl)benzyl)carbamoyl)pyrrolidin-1-yl)-3,3-dimethyl-1-oxobutan-2-yl)amino)-10-oxodecanoic acid (s-4g). (white solid, 0.96 g, 66%) ^{1}H NMR (500 MHz, $CDCl_3$) δ 8.79 (s, 1H), 7.38 (t, J = 6.0 Hz, 1H), 7.35 (s, 4H), 7.01 (d, J = 9.0 Hz, 1H), 5.80 (br, 1H), 4.68 – 4.52 (m, 4H), 4.29 (dd, J = 15.2, 5.0 Hz, 1H), 4.12 (d, J = 11.2 Hz, 1H),

3.72 – 3.62 (m, 1H), 2.51 (s, 3H), 2.41 – 2.33 (m, 1H), 2.32 – 2.23 (m, 2H), 2.23 – 2.11 (m, 3H), 1.65 – 1.48 (m, 4H), 1.32 – 1.21 (m, 8H), 0.95 (s, 9H). HRMS (ESI) m/z: cal. $C_{32}H_{47}N_4O_6S^+$ $[M+H]^+$, 615.3211; found. 615.3215.

11-(((S)-1-((2S,4R)-4-hydroxy-2-((4-(4-methylthiazol-5-yl)benzyl)carbamoyl)pyrrolidin-1-yl)-3,3-dimethyl-1-oxobutan-2-yl)amino)-11-oxoundecanoic acid (s-4h). (white solid, 1.0 g, 67%) ^{1}H NMR (500 MHz, $CDCl_3$) δ 8.77 (s, 1H), 7.39 – 7.32 (m, 4H), 7.30 (m, 1H), 7.01 (d, J = 8.8 Hz, 1H), 4.69 – 4.59 (m, 3H), 4.53 (s, 1H), 4.29 (dd, J = 15.2, 5.0 Hz, 1H), 4.14 (d, J = 11.3 Hz, 1H), 3.68 – 3.64 (m, 1H), 2.51 (s, 3H), 2.44 – 2.40 (m, 1H), 2.29 (t, J = 7.1 Hz, 2H), 2.26 – 2.12 (m, 3H), 1.68 – 1.48 (m, 4H), 1.30 – 1.20 (m, 10H), 0.95 (s, 9H). HRMS (ESI) m/z: cal. $C_{33}H_{49}N_4O_6S^+$ $[M+H]^+$, 629.3367; found. 629.3358.

3-(2-(3-(((S)-1-((2S,4R)-4-hydroxy-2-((4-(4-methylthiazol-5-yl)benzyl)carbamoyl)pyrrolidin-1-yl)-3,3-dimethyl-1-oxobutan-2-yl)amino)-3-oxopropoxy)ethoxy)propanoic acid (s-5a). (white solid, 0.53 g, 44%) ^{1}H NMR (500 MHz, DMSO) δ 12.17 (s, 1H), 8.99 (s, 1H), 8.57 (t, J = 6.0 Hz, 1H), 7.92 (d, J = 9.3 Hz, 1H), 7.41 (dd, J = 18.5, 8.2 Hz, 4H), 4.55 (d, J = 9.5 Hz, 1H), 4.46 – 4.40 (m, 2H), 4.36 (s, 1H), 4.23 (dd, J = 15.8, 5.4 Hz, 1H), 3.69 – 3.56 (m, 7H), 3.49 – 3.46 (m, 4H), 2.58 – 2.53 (m, 1H), 2.47 – 2.42 (m, 2H), 2.45 (s, 3H), 2.39 – 2.32 (m, 1H), 2.06 – 2.01 (m, 1H), 1.95 – 1.88 (m, 1H), 0.94 (s, 9H). HRMS (ESI) m/z: cal. $C_{30}H_{43}N_4O_8S^+$ $[M+H]^+$, 619.2796; found. 619.2800.

(S)-15-((2S,4R)-4-hydroxy-2-((4-(4-methylthiazol-5-yl)benzyl)carbamoyl)pyrrolidine-1-carbonyl)-16,16-dimethyl-13-oxo-4,7,10-trioxa-14-azaheptadecanoic acid (s-5b). (white solid, 0.63 g, 59%) ^{1}H NMR (500 MHz, DMSO) δ 8.99 (s, 1H), 8.57 (t, J = 6.0 Hz, 1H), 7.92 (d, J = 9.4 Hz, 1H), 7.41 (dd, J = 18.5, 8.2 Hz, 4H), 4.56 (d, J = 9.4 Hz, 1H), 4.47 – 4.41 (m, 2H), 4.36 (s, 1H), 4.23 (dd, J = 15.9, 5.5 Hz, 1H), 3.70 – 3.57 (m, 8H), 3.51 – 3.47 (m, 7H), 2.58 – 2.52 (m, 1H), 2.47 – 2.42 (m, 2H), 2.45 (s, 3H), 2.39 – 2.32 (m, 1H), 2.08 – 2.00 (m, 1H), 1.94 – 1.88 (m, 1H), 0.94 (s, 9H). HRMS (ESI) m/z: cal. $C_{32}H_{47}N_4O_9S^+$ $[M+H]^+$, 663.3058; found. 663.3067.

(S)-18-((2S,4R)-4-hydroxy-2-((4-(4-methylthiazol-5-yl)benzyl)carbamoyl)pyrrolidine-1-carbonyl)-19,19-dimethyl-16-oxo-4,7,10,13-tetraoxa-17-azaicosanoic acid (s-5c). (white solid, 0.53 g, 51%) ^{1}H NMR (500 MHz, DMSO) δ 8.98 (s, 1H), 8.56 (t, J = 6.0 Hz, 1H), 7.91 (d, J = 9.4 Hz, 1H), 7.40 (dd, J = 18.8, 8.3 Hz, 4H), 4.55 (d, J = 9.4 Hz, 1H), 4.45 – 4.40 (m, 2H), 4.35 (s, 1H), 4.22 (dd, J = 15.8, 5.5 Hz, 1H), 3.69 – 3.54 (m, 10H), 3.48 (d, J = 2.7 Hz, 9H), 2.56 – 2.52 (m, 1H), 2.45 – 2.41 (m, 2H), 2.45 (s, 3H), 2.38 – 2.32 (m, 1H), 2.06 – 2.00 (m, 1H), 1.94 – 1.88 (m, 1H),

0.93 (s, 9H). HRMS (ESI) m/z: cal. $C_{34}H_{51}N_4O_{10}S^+$ $[M+H]^+$, 707.3320; found. 707.3322.

(S)-21-((2S,4R)-4-hydroxy-2-((4-(4-methylthiazol-5-yl)benzyl)carbamoyl)pyrrolidine-1-carbonyl)-22,22-dimethyl-19-oxo-4,7,10,13,16-pentaoxa-20-azatricosanoic acid (s-5d). (white solid, 0.82 g, 85%) ^{1}H NMR (500 MHz, DMSO) δ 8.98 (s, 1H), 8.56 (d, J = 5.7 Hz, 1H), 7.91 (d, J = 9.3 Hz, 1H), 7.40 (dd, J = 18.6, 7.9 Hz, 4H), 4.55 (d, J = 9.3 Hz, 1H), 4.47 – 4.40 (m, 2H), 4.35 (s, 1H), 4.22 (dd, J = 15.7, 5.2 Hz, 1H), 3.68 – 3.56 (m, 11H), 3.51 – 3.49 (s, 9H), 2.56 – 2.53 (m, 1H), 2.45 – 2.41 (m, 5H), 2.44 (s, 3H), 2.36 (dd, J = 13.4, 7.0 Hz, 1H), 2.08 – 2.00 (m, 1H), 1.94 – 1.86 (m, 1H), 0.93 (s, 9H). HRMS (ESI) m/z: cal. $C_{36}H_{55}N_4O_{11}S^+$ $[M+H]^+$, 751.3583; found. 751.3579.

General procedure for synthesis of ALK degraders

In a 25 mL of round-bottom flask, to a stirred solution of ALK inhibitors (0.02 mmol, 1 equiv) in DMF (2 mL) were added linker **s-4** or **s-5** (0.02 mmol, 1 equiv), HOAt (0.04 mmol, 2 equiv), EDCI (0.04 mmol, 2 equiv) and NMM (0.2 mmol, 10 equiv) sequentially. Then the resulting mixture was stirred for 12 h at room temperature. The reaction was quenched with water (1.0 mL), followed by purification via preparative HPLC [C18 column, eluent (v/v)：MeCN/(H_2O+0.05%HCl) = 10% –100%] to afford the desired degraders.

(2S,4R)-1-((S)-2-(4-(4-(4-((5-chloro-4-((2-(dimethylphosphoryl)phenyl)amino)pyrimidin-2-yl)amino)-3-methoxyphenyl)piperazin-1-yl)-4-oxobutanamido)-3,3-dimethylbutanoyl)-4-hydroxy-N-(4-(4-methylthiazol-5-yl)benzyl)pyrrolidine-2-carboxamide (4). (white solid, 10.1 mg, 37%) ^{1}H NMR (500 MHz, CD_3OD) δ 9.98 (s, 1H), 8.22 (s, 1H), 8.18 (s, 1H), 7.80 - 7.45 (m, 8H), 7.39 (s, 1H), 7.13 (d, J = 8.5 Hz, 1H), 4.66 – 4.35 (m, 5H), 4.05 (s, 4H), 3.96 (s, 3H), 3.89 (d, J = 10.7 Hz, 1H), 3.80 (d, J = 8.1 Hz, 1H), 3.70 (s, 2H), 3.61 (s, 2H), 2.91 – 2.63 (m, 4H), 2.61 (s, 3H), 2.23 (s, 1H), 2.07 (s, 1H), 1.87 (d, J = 13.4 Hz, 6H), 1.05 (s, 9H). HRMS (ESI) calcd for $C_{49}H_{61}ClN_{10}O_7PS^+$ $[M+H]^+$, 999.3866; found, 999.3865.

(2S,4R)-1-((S)-2-(5-(4-(4-((5-chloro-4-((2-(dimethylphosphoryl)phenyl)amino)pyrimidin-2-yl)amino)-3-methoxyphenyl)piperazin-1-yl)-5-oxopentanamido)-3,3-dimethylbutanoyl)-4-hydroxy-N-(4-(4-methylthiazol-5-yl)benzyl)pyrrolidine-2-carboxamide (5). (white solid, 9.4 mg, 35%) ^{1}H NMR (500 MHz, CD_3OD) δ 10.00 (s, 1H), 8.25 (s, 1H), 8.14 (s, 1H), 7.79 - 7.63 (m, 3H), 7.61 - 7.46 (m, 6H), 7.22 (d, J = 8.6 Hz, 1H), 4.65 - 4.47 (m, 4H), 4.41 (d, J = 15.7 Hz, 1H), 4.07 (s, 4H), 3.97 (s, 3H), 3.93 (d, J = 11.1 Hz, 1H), 3.80 (dd, J = 11.0, 3.6 Hz, 1H), 3.74 (s, 2H), 3.66 (s, 2H), 2.60 (s, 3H), 2.53 (t, J = 7.4 Hz, 2H), 2.40 (t, J = 7.1 Hz, 2H), 2.28 – 2.20 (m, 1H), 2.11 – 2.02 (m, 1H), 2.01 – 1.92 (m, 2H), 1.87 (d, J = 13.6 Hz, 6H), 1.05 (s, 9H). HRMS (ESI) calcd for

$C_{50}H_{63}ClN_{10}O_7PS^+$ $[M+H]^+$, 1013.4023; found, 1013.4022.

(2S,4R)-1-((S)-2-(6-(4-(4-((5-chloro-4-((2-(dimethylphosphoryl)phenyl)amino)pyrimidin-2-yl)amino)-3-methoxyphenyl)piperazin-1-yl)-6-oxohexanamido)-3,3-dimethylbutanoyl)-4-hydroxy-N-(4-(4-methylthiazol-5-yl)benzyl)pyrrolidine-2-carboxamide. (6). (white solid, 11.4 mg, 42%) ^{1}H NMR (500 MHz, CD_3OD) δ 10.02 (d, *J* = 2.9 Hz, 1H), 8.26 (s, 1H), 8.13 (m 1H), 7.80 – 7.63 (m, 3H), 7.60 – 7.49 (m, 6H), 7.25 (d, *J* = 8.8 Hz, 1H), 4.64 – 4.46 (m, 4H), 4.40 (dd, *J* = 15.7, 3.7 Hz, 1H), 4.10 (s, 4H), 3.97 (s, 3H), 3.90 (d, *J* = 11.1 Hz, 1H), 3.80 (dd, *J* = 11.0, 3.9 Hz, 1H), 3.76 (s, 2H), 3.68 (s, 2H), 2.61 (s, 3H), 2.59 – 2.48 (m, 2H), 2.38 – 2.32 (m, 2H), 2.27 - 2.21(m, 1H), 2.10 - 2.03 (m, 1H), 1.87 (d, *J* = 13.6 Hz, 6H), 1.77 – 1.64 (m, 4H), 1.04 (s, 9H). HRMS (ESI) calcd for $C_{51}H_{65}ClN_{10}O_7PS^+$ $[M+H]^+$, 1027.4179; found, 1027.4171.

(2S,4R)-1-((S)-2-(7-(4-(4-((5-chloro-4-((2-(dimethylphosphoryl)phenyl)amino)pyrimidin-2-yl)amino)-3-methoxyphenyl)piperazin-1-yl)-7-oxoheptanamido)-3,3-dimethylbutanoyl)-4-hydroxy-N-(4-(4-methylthiazol-5-yl)benzyl)pyrrolidine-2-carboxamide (7). (white solid, 12.7 mg, 47%)^{1}H NMR (500 MHz, CD_3OD) δ 10.03 (d, *J* = 1.2 Hz, 1H), 8.26 (s, 1H), 8.13 (s, 1H), 7.78 - 7.65 (m, 3H), 7.61 – 7.48 (m, 6H), 7.25 (d, *J* = 8.6 Hz, 1H), 4.63 (d, *J* = 7.6 Hz, 1H), 4.59 – 4.53 (m, 2H), 4.50 (s, 1H), 4.40 (dd, *J* = 15.8, 6.4 Hz, 1H), 4.11 (s, 4H), 3.98 (s, 3H), 3.90 (d, *J* = 11.0 Hz, 1H), 3.80 (dd, *J* = 11.0, 3.7 Hz, 1H), 3.77 - 3.60 (m, 4H), 2.61 (s, 3H), 2.52 (t, *J* = 7.5 Hz, 2H), 2.36 – 2.19 (m, 3H), 2.12 - 2.04 (m, 1H), 1.87 (d, *J* = 13.6 Hz, 6H), 1.72 – 1.57 (m, 4H), 1.47 – 1.29 (m, 2H), 1.03 (s, 9H). HRMS (ESI) calcd for $C_{52}H_{67}ClN_{10}O_7PS^+$ $[M+H]^+$, 1041.4336; found, 1041.4346.

(2S,4R)-1-((S)-2-(8-(4-(4-((5-chloro-4-((2-(dimethylphosphoryl)phenyl)amino)pyrimidin-2-yl)amino)-3-methoxyphenyl)piperazin-1-yl)-8-oxooctanamido)-3,3-dimethylbutanoyl)-4-hydroxy-N-(4-(4-methylthiazol-5-yl)benzyl)pyrrolidine-2-carboxamide (8). (white solid, 6.8 mg, 25%) ^{1}H NMR (500 MHz, CD_3OD) δ 9.99 (d, *J* = 4.4 Hz, 1H), 8.23 (s, 1H), 8.18 (s, 1H), 7.74 (dd, *J* = 13.0, 7.6 Hz, 1H), 7.66 (t, *J* = 7.5 Hz, 2H), 7.60 – 7.46 (m, 5H), 7.40 (s, 1H), 7.14 (d, *J* = 8.7 Hz, 1H), 4.63 (d, *J* = 6.1 Hz, 1H), 4.60 -- 4.52 (m, 2H), 4.50 (s, 1H), 4.40 (dd, *J* = 15.8, 7.7 Hz, 1H), 4.05 (s, 4H), 3.96 (s, 3H), 3.91 (d, *J* = 11.0 Hz, 1H), 3.80 (dd, *J* = 11.1, 3.7 Hz, 1H), 3.68 (s, 2H), 3.62 (s, 2H), 2.61 (s, 3H), 2.51 (t, *J* = 7.5 Hz, 2H), 2.40 – 2.17 (m, 3H), 2.11 - 2.03 (m, 1H), 1.87 (d, *J* = 13.5 Hz, 6H), 1.70 – 1.55 (m, 4H), 1.45 - 1.30 (m, 4H), 1.04 (s, 9H). HRMS (ESI) calcd for $C_{53}H_{69}ClN_{10}O_7PS^+$ $[M+H]^+$, 1055.4492; found, 1055.4486.

(2S,4R)-1-((S)-2-(9-(4-(4-((5-chloro-4-((2-(dimethylphosphoryl)phenyl)amino)pyrimidin-2-yl)amino)-3-methoxyphenyl)piperazin-1-yl)-9-oxononanamido)-3,3-dimethylbutanoyl)-4-hydrox

y-N-(4-(4-methylthiazol-5-yl)benzyl)pyrrolidine-2-carboxamide (9). (white solid, 8.3 mg, 31%) ^{1}H NMR (500 MHz, CD_3OD) δ 9.96 (s, 1H), 8.19 (d, *J* = 14.1 Hz, 2H), 7.73 (dd, *J* = 14.0, 6.8 Hz, 1H), 7.67 – 7.45 (m, 6H), 7.31 (s, 1H), 7.07 (d, *J* = 8.7 Hz, 1H), 4.64 (s, 1H), 4.60 - 4.52 (m, 2H), 4.50 (s, 1H), 4.41 (d, *J* = 15.8 Hz, 1H), 4.00 (s, 4H), 3.95 (s, 3H), 3.91 (d, *J* = 11.1 Hz, 1H), 3.80 (dd, *J* = 11.0, 3.8 Hz, 1H), 3.63 (s, 2H), 3.57 (s, 2H), 2.60 (s, 3H), 2.50 (t, *J* = 7.6 Hz, 2H), 2.37 – 2.18 (m, 3H), 2.11 - 2.03 (m, 1H), 1.87 (d, *J* = 13.6 Hz, 6H), 1.70 – 1.55 (m, 4H), 1.45 - 1.30 (m, 6H), 1.02 (s, 9H). HRMS (ESI) calcd for $C_{54}H_{71}ClN_{10}O_7PS^+$ $[M+H]^+$, 1069.4649; found, 1069.4642.

(2S,4R)-1-((S)-2-(10-(4-(4-((5-chloro-4-((2-(dimethylphosphoryl)phenyl)amino)pyrimidin-2-yl)amino)-3-methoxyphenyl)piperazin-1-yl)-10-oxodecanamido)-3,3-dimethylbutanoyl)-4-hydroxy-N-(4-(4-methylthiazol-5-yl)benzyl)pyrrolidine-2-carboxamide (10). (white solid, 10.6 mg, 39%) ^{1}H NMR (500 MHz, CD_3OD) δ 9.56 (d, *J* = 4.2 Hz, 1H), 8.35 (s, 1H), 8.08 (s, 1H), 7.70 (s, 1H), 7.62 - 7.30 (m, 6H), 6.86 (s, 1H), 6.71 (s, 1H), 4.64 (d, *J* = 3.5 Hz, 1H), 4.60 - 4.47 (m, 3H), 4.39 (dd, *J* = 15.7, 3.2 Hz, 1H), 4.00 – 3.69 (m, 9H), 3.36 (s, 4H), 2.55 (d, *J* = 3.8 Hz, 3H), 2.51 – 2.40 (m, 2H), 2.38 - 2.18 (m, 3H), 2.12 – 2.02 (m, 1H), 1.89 (dd, *J* = 13.6, 3.5 Hz, 6H), 1.62 (s, 4H), 1.35 (s, 8H), 1.03 (s, 9H). HRMS (ESI) calcd for $C_{55}H_{73}ClN_{10}O_7PS^+$ $[M+H]^+$, 1083.4805; found, 1083.4802.

N1-(1-(4-((5-chloro-4-((2-(dimethylphosphoryl)phenyl)amino)pyrimidin-2-yl)amino)-3-methoxyphenyl)piperidin-4-yl)-N4-((S)-1-((2S,4R)-4-hydroxy-2-((4-(4-methylthiazol-5-yl)benzyl)carbamoyl)pyrrolidin-1-yl)-3,3-dimethyl-1-oxobutan-2-yl)succinamide (11). (white solid, 12.8 mg, 63%) ^{1}H NMR (500 MHz, CD_3OD) *δ* 9.95 (s, 1H), 8.27 (s, 1H), 8.11 (s, 1H), 7.78 – 7.73 (m, 2H), 7.68 (t, *J* = 7.5 Hz, 1H), 7.60 – 7.50 (m, 6H), 7.29 (d, *J* = 8.2 Hz, 1H), 4.62 – 4.47 (m, 4H), 4.41 (d, *J* = 15.6 Hz, 1H), 4.19 – 4.11 (m, 1H), 4.00 (s, 3H), 3.91 – 3.89 (m, 1H), 3.81 – 3.78 (m, 5H), 2.67 – 2.53 (m, 4H), 2.59 (s, 3H), 2.31 – 2.15 (m, 5H), 2.11 – 2.04 (m, 1H), 1.88 (s, 3H), 1.86 (s, 3H), 1.04 (s, 9H). HRMS (ESI) calcd for $C_{50}H_{63}ClN_{10}O_7PS^+$ $[M+H]^+$: 1013.4023, found 1013.4017.

N1-(1-(4-((5-chloro-4-((2-(dimethylphosphoryl)phenyl)amino)pyrimidin-2-yl)amino)-3-methoxyphenyl)piperidin-4-yl)-N5-((S)-1-((2S,4R)-4-hydroxy-2-((4-(4-methylthiazol-5-yl)benzyl)carbamoyl)pyrrolidin-1-yl)-3,3-dimethyl-1-oxobutan-2-yl)glutaramide (12). (white solid, 12.2 mg, 59%). ^{1}H NMR (500 MHz, CD_3OD) *δ* 9.96 (s, 1H), 8.28 (s, 1H), 8.11 (s, 1H), 7.78 – 7.73 (m, 2H), 7.68 (t, *J* = 7.8 Hz, 1H), 7.61 – 7.56 (m, 3H), 7.55 – 7.49 (m, 3H), 7.30 (d, *J* = 8.7 Hz, 1H), 4.64 (s, 1H), 4.69 – 4.51 (m, 3H), 4.45 – 4.40 (m, 1H), 4.20 – 4.12 (m, 1H), 4.00 (s, 3H), 3.93 (d, *J* = 11.2 Hz, 1H), 3.86 – 3.73 (m, 5H), 2.60 (s, 3H), 2.38 – 2.17 (m, 9H), 2.11 – 2.05 (m, 1H), 1.96 – 1.91 (m,

2H), 1.88 (s, 3H), 1.85 (s, 3H), 1.05 (s, 9H). HRMS (ESI) calcd for $C_{51}H_{65}ClN_{10}O_7PS^+$ $[M+H]^+$: 1027.4179, found 1027.4170.

N1-(1-(4-((5-chloro-4-((2-(dimethylphosphoryl)phenyl)amino)pyrimidin-2-yl)amino)-3-methoxyphenyl)piperidin-4-yl)-N6-((S)-1-((2S,4R)-4-hydroxy-2-((4-(4-methylthiazol-5-yl)benzyl)carbamoyl)pyrrolidin-1-yl)-3,3-dimethyl-1-oxobutan-2-yl)adipamide

(13). (white solid, 13.1 mg, 63%) ^{1}H NMR (500 MHz, CD_3OD) δ 10.01 (s, 1H), 8.28 (s, 1H), 8.11 (s, 1H), 7.78 – 7.74 (m, 2H), 7.69 (t, J = 7.9 Hz, 1H), 7.63 (s, 1H), 7.59 – 7.57 (m, 2H), 7.55 – 7.50 (m, 3H), 7.32 (d, J = 6.9 Hz, 1H), 4.64 (s, 1H), 4.61 – 4.47 (m, 3H), 4.43 – 4.39 (m, 1H), 4.21 – 4.13 (m, 1H), 4.00 (s, 3H), 3.92 (d, J = 11.1 Hz, 1H), 3.85 – 3.71 (m, 5H), 2.61 (s, 3H), 2.36 – 2.17 (m, 9H), 2.10 – 2.04 (m, 1H), 1.88 (s, 3H), 1.86 (s, 3H), 1.70 – 1.62 (m, 4H), 1.04 (s, 9H). HRMS (ESI) calcd for $C_{52}H_{67}ClN_{10}O_7PS^+$ $[M+H]^+$: 1041.4336, found 1041.4339.

N1-(1-(4-((5-chloro-4-((2-(dimethylphosphoryl)phenyl)amino)pyrimidin-2-yl)amino)-3-methoxyphenyl)piperidin-4-yl)-N7-((S)-1-((2S,4R)-4-hydroxy-2-((4-(4-methylthiazol-5-yl)benzyl)carbamoyl)pyrrolidin-1-yl)-3,3-dimethyl-1-oxobutan-2-yl)heptanediamide (14). (white solid, 12.3 mg, 58%) ^{1}H NMR (500 MHz, CD_3OD) δ 9.97 (s, 1H), 8.27 (s, 1H), 8.11 (s, 1H), 7.77 – 7.73 (m, 2H), 7.68 (t, J = 7.8 Hz, 1H), 7.61 – 7.50 (m, 6H), 7.29 (d, J = 8.7 Hz, 1H), 4.64 (s, 1H), 4.61 – 4.48 (m, 3H), 4.44 – 4.38 (m, 1H), 4.18 – 4.12 (m, 1H), 4.00 (s, 3H), 3.91 (d, J = 11.1 Hz, 1H), 3.85 – 3.70 (m, 5H), 2.60 (s, 3H), 2.36 – 2.15 (m, 9H), 2.10 – 2.05 (m, 1H), 1.88 (s, 3H), 1.85 (s, 3H), 1.69 – 1.61 (m, 4H), 1.42 – 1.33 (m, 2H), 1.04 (s, 9H). HRMS (ESI) calcd for $C_{53}H_{69}ClN_{10}O_7PS^+$ $[M+H]^+$: 1055.4492, found 1055.4491.

N1-(1-(4-((5-chloro-4-((2-(dimethylphosphoryl)phenyl)amino)pyrimidin-2-yl)amino)-3-methoxyphenyl)piperidin-4-yl)-N8-((S)-1-((2S,4R)-4-hydroxy-2-((4-(4-methylthiazol-5-yl)benzyl)carbamoyl)pyrrolidin-1-yl)-3,3-dimethyl-1-oxobutan-2-yl)octanediamide

(15). (white solid, 14.8 mg, 69%) ^{1}H NMR (500 MHz, CD_3OD) δ 9.91 (s, 1H), 8.27 (s, 1H), 8.11 (s, 1H), 7.77 – 7.73 (m, 2H), 7.69 (t, J = 7.8 Hz, 1H), 7.61 (d, J = 2.1 Hz, 1H), 7.58 – 7.51 (m, 5H), 7.31 (d, J = 8.7 Hz, 1H), 4.64 (s, 1H), 4.60 – 4.49 (m, 3H), 4.43 – 4.38 (m, 1H), 4.20 – 4.13 (m, 1H), 4.00 (s, 3H), 3.92 (d, J = 11.1 Hz, 1H), 3.86 – 3.75 (m, 5H), 2.60 (s, 3H), 2.33 – 2.18 (m, 9H), 2.11 – 2.05 (m, 1H), 1.88 (s, 3H), 1.85 (s, 3H), 1.68 – 1.59 (m, 4H), 1.41 – 1.34 (m, 4H), 1.04 (s, 9H). HRMS (ESI) calcd for $C_{54}H_{71}ClN_{10}O_7PS^+$ $[M+H]^+$: 1069.4649, found 1069.4661.

N1-(1-(4-((5-chloro-4-((2-(dimethylphosphoryl)phenyl)amino)pyrimidin-2-yl)amino)-3-methoxyphenyl)piperidin-4-yl)-N9-((S)-1-((2S,4R)-4-hydroxy-2-((4-(4-methylthiazol-5-yl)benzyl)car

bamoyl)pyrrolidin-1-yl)-3,3-dimethyl-1-oxobutan-2-yl)nonanediamide (16). (white solid, 12.8 mg, 59%) ^{1}H NMR (500 MHz, CD_3OD) δ 10.01 (s, 1H), 8.28 (s, 1H), 8.11 (s, 1H), 7.78 – 7.73 (m, 2H), 7.69 (t, *J* = 7.9 Hz, 1H), 7.63 (d, *J* = 2.0 Hz, 1H), 7.60 – 7.57 (m, 2H), 7.55 – 7.49 (m, 3H), 7.31 (d, *J* = 8.8 Hz, 1H), 4.64 (s, 1H), 4.60 – 4.49 (m, 3H), 4.44 – 4.38 (m, 1H), 4.21 – 4.13 (m, 1H), 4.00 (s, 3H), 3.91 (d, *J* = 11.1 Hz, 1H), 3.85 – 2.73 (m, 5H), 2.61 (s, 3H), 2.33 – 2.18 (m, 9H), 2.10 – 2.04 (m, 1H), 1.88 (s, 3H), 1.86 (s, 3H), 1.66 – 1.59 (m, 4H), 1.36 (s, 6H), 1.04 (s, 9H). HRMS (ESI) calcd for $C_{55}H_{73}ClN_{10}O_7PS^+$ $[M+H]^+$: 1083.4805, found 1083.4797.

N1-(1-(4-((5-chloro-4-((2-(dimethylphosphoryl)phenyl)amino)pyrimidin-2-yl)amino)-3-methoxyphenyl)piperidin-4-yl)-N10-((S)-1-((2S,4R)-4-hydroxy-2-((4-(4-methylthiazol-5-yl)benzyl)carbamoyl)pyrrolidin-1-yl)-3,3-dimethyl-1-oxobutan-2-yl)decanediamide (17). (white solid, 10.2 mg, 46%) ^{1}H NMR (500 MHz, CD_3OD) δ 10.02 (s, 1H), 8.28 (s, 1H), 8.11 (s, 1H), 7.79 – 7.73 (m, 2H), 7.69 (t, *J* = 7.9 Hz, 1H), 7.63 (d, *J* = 2.0 Hz, 1H), 7.58 (d, *J* = 8.3 Hz, 2H), 7.54 – 7.50 (m, 3H), 7.32 (d, *J* = 8.6 Hz, 1H), 4.64 (s, 1H), 4.60 – 4.49 (m, 3H), 4.44 – 4.38 (m, 1H), 4.20 – 4.14 (m, 1H), 4.00 (s, 3H), 3.91 (d, *J* = 11.2 Hz, 1H), 3.81 (dd, *J* = 10.9, 3.9 Hz, 5H), 2.61 (s, 3H), 2.33 – 2.18 (m, 9H), 2.10 – 2.05 (m, 1H), 1.88 (s, 3H), 1.86 (s, 3H), 1.67 – 1.57 (m, 4H), 1.35 (s, 9H), 1.04 (s, 9H). HRMS (ESI) calcd for $C_{56}H_{75}ClN_{10}O_7PS^+$ $[M+H]^+$: 1097.4962, found 1097.4953.

N1-(1-(4-((5-chloro-4-((2-(dimethylphosphoryl)phenyl)amino)pyrimidin-2-yl)amino)-3-methoxyphenyl)piperidin-4-yl)-N11-((S)-1-((2S,4R)-4-hydroxy-2-((4-(4-methylthiazol-5-yl)benzyl)carbamoyl)pyrrolidin-1-yl)-3,3-dimethyl-1-oxobutan-2-yl)undecanediamide (18, SIAIS117). (white solid, 10.6 mg, 48%) ^{1}H NMR (500 MHz, CD_3OD) δ 8.84 (s, 1H), 8.31 (dd, *J* = 7.5, 3.9 Hz, 1H), 8.02 (s, 1H), 7.77 (d, *J* = 8.6 Hz, 1H), 7.62-7.58 (m, 1H), 7.53 (t, *J* = 7.8 Hz, 1H), 7.43 (t, *J* = 7.3 Hz, 2H), 7.37 (d, *J* = 7.9 Hz, 2H), 7.28 (t, *J* = 7.2 Hz, 1H), 6.84 (s, 1H), 6.64 (s, 1H), 4.64 (s, 1H), 4.59 (t, *J* = 8.3 Hz, 1H), 4.51 (d, *J* = 15.4 Hz, 2H), 4.34 (d, *J* = 15.5 Hz, 1H), 3.93 – 3.83 (m, 5H), 3.81-3.78 (m, 1H), 3.74 – 3.57 (m, 2H), 3.04-2.85 (m, 2H), 2.44 (s, 3H), 2.28 – 2.18 (m, 4H), 2.10 – 2.02 (m, 2H), 1.83 (d, *J* = 13.5 Hz, 6H), 1.80-1.76 (m, 2H), 1.60 (d, *J* = 6.4 Hz, 4H), 1.38 (d, *J* = 7.0 Hz, 2H), 1.33-1.28 (m, 10H), 1.03 (s, 9H). ^{13}C NMR (126 MHz, CD_3OD) δ 176.24, 176.15, 174.56, 172.16, 159.98, 156.85, 152.34, 142.71, 142.13, 141.92, 141.17, 137.74, 134.32, 132.60, 132.52, 130.44, 129.47, 127.69, 127.11, 114.44, 108.03, 106.63, 71.04, 60.81, 59.04, 57.97, 57.52, 43.55, 38.98, 36.90, 36.54, 30.41, 30.34, 30.24, 30.21, 27.04, 27.00, 18.37, 17.80, 12.95. HRMS (ESI) calcd for $C_{57}H_{77}ClN_{10}O_7PS$ $[M+H]^+$: 1111.5118, found 1111.5109.

(2S,4R)-1-((S)-2-(4-(4-(1-(4-((5-chloro-4-((2-(dimethylphosphoryl)phenyl)amino)pyrimidin-2

-yl)amino)-3-methoxyphenyl)piperidin-4-yl)piperazin-1-yl)-4-oxobutanamido)-3,3-dimethylbutanoyl)-4-hydroxy-N-(4-(4-methylthiazol-5-yl)benzyl)pyrrolidine-2-carboxamide (19). (white solid, 9.1 mg, 48%) ^{1}H NMR (500 MHz, CD_3OD) δ 9.62 (s, 1H), 8.31 (s, 1H), 8.11 (s, 1H), 7.70 (dd, *J* = 14.0, 9.1 Hz, 1H), 7.60 (s, 1H), 7.54 (d, *J* = 8.2 Hz, 2H), 7.49 (d, *J* = 8.3 Hz, 2H), 7.43 (t, *J* = 7.7 Hz, 2H), 6.98 (s, 1H), 6.80 (s, 1H), 4.61 (s, 1H), 4.59-4.54 (m, 2H), 4.50 (s, 1H), 4.40 (d, *J* = 15.8 Hz, 1H), 4.34 – 4.22 (m, 1H), 3.97 (d, *J* = 11.9 Hz, 2H), 3.92 – 3.86 (m, 4H), 3.81 (dd, *J* = 11.0, 3.9 Hz, 1H), 3.67-3.60 (m, 5H), 3.17 (s, 4H), 2.84 – 2.57 (m, 5H), 2.56 (s, 3H), 2.37 (d, *J* = 10.3 Hz, 2H), 2.28 – 2.19 (m, 1H), 2.19 – 2.05 (m, 3H), 1.88 (d, *J* = 13.6 Hz, 6H), 1.03 (s, 9H). HRMS (ESI) calcd for $C_{54}H_{70}ClN_{11}O_7PS$ $[M+H]^+$: 1082.4601, found 1082.4593.

(2S,4R)-1-((S)-2-(5-(4-(1-(4-((5-chloro-4-((2-(dimethylphosphoryl)phenyl)amino)pyrimidin-2-yl)amino)-3-methoxyphenyl)piperidin-4-yl)piperazin-1-yl)-5-oxopentanamido)-3,3-dimethylbutanoyl)-4-hydroxy-N-(4-(4-methylthiazol-5-yl)benzyl)pyrrolidine-2-carboxamide (20). (white solid, 6.3 mg, 33%) ^{1}H NMR (500 MHz, CD_3OD) δ 9.72 (s, 1H), 8.28 (s, 1H), 8.15 (s, 1H), 7.72 (dd, *J* = 13.9, 7.9 Hz, 1H), 7.67 – 7.60 (m, 1H), 7.59 – 7.35 (m, 6H), 7.14 (s, 1H), 6.91 (s, 1H), 4.69 – 4.49 (m, 5H), 4.41 (d, *J* = 15.8 Hz, 1H), 4.31 – 4.16 (m, 1H), 3.95-3.92 (m, 6H), 3.81 (d, *J* = 7.8 Hz, 1H), 3.69 (s, 4H), 3.27 – 3.02 (m, 5H), 2.57 (s, 3H), 2.44-2.37 (m, 6H), 2.24-2.08 (m, 4H), 1.93-1.87 (m, 8H), 1.04 (s, 9H). HRMS (ESI) calcd for $C_{55}H_{72}ClN_{11}O_7PS$ $[M+H]^+$: 1096.4758, found 1096.4748.

(2S,4R)-1-((S)-2-(6-(4-(1-(4-((5-chloro-4-((2-(dimethylphosphoryl)phenyl)amino)pyrimidin-2-yl)amino)-3-methoxyphenyl)piperidin-4-yl)piperazin-1-yl)-6-oxohexanamido)-3,3-dimethylbutanoyl)-4-hydroxy-N-(4-(4-methylthiazol-5-yl)benzyl)pyrrolidine-2-carboxamide (21). (white solid, 8.6 mg, 44%) ^{1}H NMR (500 MHz, CD_3OD) δ 9.76 (s, 1H), 8.26 (s, 1H), 8.15 (s, 1H), 7.72 (dd, *J* = 13.9, 7.8 Hz, 1H), 7.63 (t, *J* = 8.0 Hz, 1H), 7.59 – 7.43 (m, 6H), 7.17 (s, 1H), 6.95 (s, 1H), 4.64 (s, 1H), 4.61 – 4.49 (m, 3H), 4.41 (d, *J* = 15.6 Hz, 1H), 4.25 (s, 1H), 3.99 – 3.88 (m, 6H), 3.81 (dd, *J* = 10.8, 3.8 Hz, 1H), 3.69 (s, 4H), 3.40-3.31 (m, 3H), 3.17 (s, 3H), 2.58 (s, 3H), 2.50-2.43 (m, 4H), 2.36-2.22 (m, 5H), 2.13 – 2.03 (m, 1H), 1.88 (d, *J* = 13.6 Hz, 6H), 1.67 (s, 4H), 1.05 (s, 9H). HRMS (ESI) calcd for $C_{56}H_{74}ClN_{11}O_7PS$ $[M+H]^+$: 1110.4914, found 1110.4903.

(2S,4R)-1-((S)-2-(7-(4-(1-(4-((5-chloro-4-((2-(dimethylphosphoryl)phenyl)amino)pyrimidin-2-yl)amino)-3-methoxyphenyl)piperidin-4-yl)piperazin-1-yl)-7-oxoheptanamido)-3,3-dimethylbutanoyl)-4-hydroxy-N-(4-(4-methylthiazol-5-yl)benzyl)pyrrolidine-2-carboxamide (22). (white solid, 8.4 mg, 43%) ^{1}H NMR (500 MHz, CD_3OD) δ 9.64 (s, 1H), 8.32 (s, 1H), 8.11 (s, 1H), 7.71 (dd,

J = 13.9, 7.7 Hz, 1H), 7.61 (s, 1H), 7.55-7.44 (m, 6H), 7.01 (s, 1H), 6.81 (s, 1H), 4.64 (s, 1H), 4.60-4.50 (m, 3H), 4.41 (d, *J* = 15.7 Hz, 1H), 3.96 (d, *J* = 10.3 Hz, 2H), 3.92-3.90 (m, 4H), 3.81 (dd, *J* = 10.9, 3.9 Hz, 1H), 3.69-3.60 (m, 4H), 3.31-3.17 (m, 7H), 2.56 (s, 3H), 2.47 (t, *J* = 7.3 Hz, 2H), 2.37 (s, 2H), 2.35 – 2.27 (m, 2H), 2.27 – 2.20 (m, 1H), 2.19 – 2.03 (m, 3H), 1.88 (d, *J* = 13.6 Hz, 6H), 1.70 – 1.59 (m, 4H), 1.43-1.37 (m, 2H), 1.03 (s, 9H). HRMS (ESI) calcd for $C_{57}H_{76}ClN_{11}O_7PS$ $[M+H]^+$: 1124.5071, found 1124.5070.

(2S,4R)-1-((S)-2-(8-(4-(1-(4-((5-chloro-4-((2-(dimethylphosphoryl)phenyl)amino)pyrimidin-2-yl)amino)-3-methoxyphenyl)piperidin-4-yl)piperazin-1-yl)-8-oxooctanamido)-3,3-dimethylbutanoyl)-4-hydroxy-N-(4-(4-methylthiazol-5-yl)benzyl)pyrrolidine-2-carboxamide (23). (white solid, 8.3 mg, 42%) ^{1}H NMR (500 MHz, CD_3OD) δ 9.76 (s, 1H), 8.27 (s, 1H), 8.15 (s, 1H), 7.72 (dd, *J* = 14.0, 7.9 Hz, 1H), 7.63 (s, 1H), 7.59 – 7.39 (m, 6H), 7.19 (s, 1H), 6.94 (s, 1H), 4.64 (s, 1H), 4.62 – 4.46 (m, 3H), 4.41 (d, *J* = 15.7 Hz, 1H), 4.26 (s, 1H), 4.03 – 3.86 (m, 6H), 3.81 (dd, *J* = 10.9, 3.8 Hz, 1H), 3.69 (s, 4H), 3.33 (s, 3H), 3.17 (s, 3H), 2.58 (s, 3H), 2.53 – 2.38 (m, 4H), 2.38 – 2.17 (m, 5H), 2.13 – 2.02 (m, 1H), 1.88 (d, *J* = 13.6 Hz, 6H), 1.64 (d, *J* = 6.7 Hz, 4H), 1.39 (d, *J* = 3.5 Hz, 4H), 1.03 (s, 9H). HRMS (ESI) calcd for $C_{58}H_{78}ClN_{11}O_7PS$ $[M+H]^+$: 1138.5227, found 1138.5230.

(2S,4R)-1-((S)-2-(9-(4-(1-(4-((5-chloro-4-((2-(dimethylphosphoryl)phenyl)amino)pyrimidin-2-yl)amino)-3-methoxyphenyl)piperidin-4-yl)piperazin-1-yl)-9-oxononanamido)-3,3-dimethylbutanoyl)-4-hydroxy-N-(4-(4-methylthiazol-5-yl)benzyl)pyrrolidine-2-carboxamide (24). (white solid, 8.9 mg, 44%) ^{1}H NMR (500 MHz, CD_3OD) δ 9.82 – 9.70 (m, 1H), 8.25 (s, 1H), 8.16 (s, 1H), 7.78 – 7.68 (m, 1H), 7.64 (s, 1H), 7.56-7.47 (m, 6H), 7.23 (s, 1H), 6.98 (s, 1H), 4.64 (s, 1H), 4.61 – 4.47 (m, 3H), 4.40 (d, *J* = 15.7 Hz, 1H), 4.25 (s, 1H), 3.92 (t, *J* = 8.1 Hz, 6H), 3.81 (dd, *J* = 11.0, 3.8 Hz, 1H), 3.70 (s, 4H), 3.39-3.32 (m, 3H), 3.30-3.17 (m, 3H), 2.58 (s, 3H), 2.52 – 2.39 (m, 4H), 2.39 – 2.17 (m, 5H), 2.13 – 2.03 (m, 1H), 1.88 (d, *J* = 13.6 Hz, 6H), 1.62 (s, 4H), 1.37 (s, 6H), 1.03 (s, 9H). HRMS (ESI) calcd for $C_{59}H_{80}ClN_{11}O_7PS$ $[M+H]^+$: 1152.5384, found 1152.5388.

(2S,4R)-1-((S)-2-(10-(4-(1-(4-((5-chloro-4-((2-(dimethylphosphoryl)phenyl)amino)pyrimidin-2-yl)amino)-3-methoxyphenyl)piperidin-4-yl)piperazin-1-yl)-10-oxodecanamido)-3,3-dimethylbutanoyl)-4-hydroxy-N-(4-(4-methylthiazol-5-yl)benzyl)pyrrolidine-2-carboxamide (25). (white solid, 7.7 mg, 38%) ^{1}H NMR (500 MHz, CD_3OD) δ 9.88 – 9.79 (m, 1H), 8.19 (s, 2H), 7.73 (dd, *J* = 13.9, 7.8 Hz, 1H), 7.65 (s, 1H), 7.57-7.48 (m, 6H), 7.33 (s, 1H), 7.06 (s, 1H), 4.64 (s, 1H), 4.61 – 4.46 (m, 3H), 4.44 – 4.37 (m, 1H), 4.27 (s, 1H), 3.95-3.90 (m, 6H), 3.85 – 3.48 (m, 8H), 3.20-3.04 (m, 3H), 2.60 (s, 3H), 2.53 – 2.43 (m, 4H), 2.42 – 2.19 (m, 5H), 2.10-2.05 (m, 1H), 1.88 (d, *J* = 13.6

Hz, 6H), 1.62 (d, *J* = 7.0 Hz, 4H), 1.36 (s, 8H), 1.03 (s, 9H). HRMS (ESI) calcd for $C_{60}H_{82}ClN_{11}O_7PS$ $[M+H]^+$: 1166.5540, found 1166.5528.

(2S,4R)-1-((S)-2-(3-(2-(3-(4-(4-((5-chloro-4-((2-(dimethylphosphoryl)phenyl)amino) pyrimidin-2-yl)amino)-3-methoxyphenyl)piperazin-1-yl)-3-oxopropoxy)ethoxy) propanamido)-3,3-dimethylbutanoyl)-4-hydroxy-N-(4-(4-methylthiazol-5-yl)benzyl) pyrrolidine-2-carboxamide (26). (white solid, 14.9 mg, 55%) ^{1}H NMR (500 MHz, CD_3OD) δ 8.89 (s, 1H), 8.40 (s, 1H), 8.03 (s, 1H), 7.66 (dd, *J* = 14.0, 7.7 Hz, 1H), 7.55 (s, 1H), 7.46 (d, *J* = 8.2 Hz, 2H), 7.42 - 7.33 (m, 3H), 7.29 (d, *J* = 7.8 Hz, 1H), 6.72 (s, 1H), 6.58 (d, *J* = 8.5 Hz, 1H), 4.64 (s, 1H), 4.60 – 4.52 (m, 2H), 4.49 (s, 1H), 4.34 (d, *J* = 15.5 Hz, 1H), 3.88 (d, *J* = 10.9 Hz, 1H), 3.84 (s, 3H), 3.81 – 3.66 (m, 9H), 3.62 – 3.58 (m, 4H), 3.31 (s, 2H), 3.21 (s, 2H), 2.77 – 2.66 (m, 2H), 2.46 (s, 3H), 2.51 – 2.43 (m, 1H), 2.43 – 2.36 (m, 1H), 2.25 - 2.18 (m, 1H), 2.12 - 2.04 (m, 1H), 1.88 (d, *J* = 13.6 Hz, 6H), 1.03 (s, 9H). HRMS (ESI) calcd for $C_{53}H_{69}ClN_{10}O_9PS^+$ $[M+H]^+$, 1087.4390; found, 1087.4388.

(2S,4R)-1-((S)-2-(tert-butyl)-16-(4-(4-((5-chloro-4-((2-(dimethylphosphoryl)phenyl)amino)py rimidin-2-yl)amino)-3-methoxyphenyl)piperazin-1-yl)-4,16-dioxo-7,10,13-trioxa-3-azahexadec anoyl)-4-hydroxy-N-(4-(4-methylthiazol-5-yl)benzyl)pyrrolidine-2-carboxamide (27). (white solid, 17.1 mg, 63%) ^{1}H NMR (500 MHz, CD_3OD) δ 8.91 (s, 1H), 8.39 (s, 1H), 8.04 (s, 1H), 7.66 (dd, *J* = 14.1, 7.8 Hz, 1H), 7.54 (s, 1H), 7.46 (d, *J* = 8.2 Hz, 2H), 7.44 – 7.35 (m, 3H), 7.29 (d, *J* = 8.2 Hz, 1H), 6.73 (d, *J* = 2.1 Hz, 1H), 6.59 (d, *J* = 8.4 Hz, 1H), 4.64 (s, 1H), 4.59 – 4.51 (m, 2H), 4.49 (s, 1H), 4.35 (d, *J* = 15.5 Hz, 1H), 3.88 (d, *J* = 11.1 Hz, 1H), 3.85 (s, 3H), 3.82 – 3.73 (m, 7H), 3.72 – 3.65 (m, 2H), 3.63 – 3.54 (m, 8H), 3.44 (t, *J* = 7.0 Hz, 1H), 3.31 (s, 2H),3.24 (s, 2H), 2.71 (t, *J* = 6.2 Hz, 2H), 2.60 – 2.50 (m, 1H), 2.47 (s, 3H), 2.49 – 2.40 (m, 1H), 2.25 - 2.18 (m, 1H), 2.11 – 2.05 (m, 1H), 1.88 (d, *J* = 13.6 Hz, 6H), 1.03 (s, 9H). HRMS (ESI) calcd for $C_{55}H_{73}ClN_{10}O_{10}PS^+$ $[M+H]^+$, 1131.4652; found, 1131.4651.

(2S,4R)-1-((S)-2-(tert-butyl)-19-(4-(4-((5-chloro-4-((2-(dimethylphosphoryl)phenyl)amino)py rimidin-2-yl)amino)-3-methoxyphenyl)piperazin-1-yl)-4,19-dioxo-7,10,13,16-tetraoxa-3-azanon adecanoyl)-4-hydroxy-N-(4-(4-methylthiazol-5-yl)benzyl)pyrrolidine-2-carboxamide (28). (white solid, 16.7 mg, 62%) ^{1}H NMR (500 MHz, CD_3OD) δ 8.89 (s, 1H), 8.39 (s, 1H), 8.04 (s, 1H), 7.66 (dd, *J* = 13.5, 8.1 Hz, 1H), 7.54 (s, 1H), 7.46 (d, *J* = 8.1 Hz, 2H), 7.42 - 7.35 (m, 3H), 7.31 (d, *J* = 8.6 Hz, 1H), 6.73 (s, 1H), 6.58 (d, *J* = 7.5 Hz, 1H), 4.64 (s, 1H), 4.59 – 4.50 (m, 2H), 4.49 (s, 1H), 4.35 (d, *J* = 15.5 Hz, 1H), 3.87 (d, *J* = 12.2 Hz, 1H), 3.85 (s, 3H), 3.82 – 3.72 (m, 7H), 3.73 - 3.65

(m, 2H), 3.64 – 3.53 (m, 12H), 3.31 (s, 2H),3.24 (s, 2H), 2.72 (t, *J* = 6.2 Hz, 2H), 2.59 – 2.51 (m, 1H), 2.46 (s, 3H), 2.49 – 2.40 (m, 1H), 2.25 – 2.16 (m, 1H), 2.11 -2.04 (m, 1H), 1.88 (d, *J* = 13.6 Hz, 6H), 1.03 (s, 9H). HRMS (ESI) calcd for $C_{57}H_{77}ClN_{10}O_{11}PS^+$ $[M+H]^+$, 1175.4915; found, 1175.4918.

(2S,4R)-1-((S)-2-(tert-butyl)-22-(4-(4-((5-chloro-4-((2-(dimethylphosphoryl)phenyl)amino)pyrimidin-2-yl)amino)-3-methoxyphenyl)piperazin-1-yl)-4,22-dioxo-7,10,13,16,19-pentaoxa-3-azadocosanoyl)-4-hydroxy-N-(4-(4-methylthiazol-5-yl)benzyl)pyrrolidine-2-carboxamide (29). (white solid, 16.5 mg, 61%) ^{1}H NMR (500 MHz, CD_3OD) δ 8.90 (s, 1H), 8.39 (s, 1H), 8.03 (s, 1H), 7.67 (dd, *J* = 14.0, 6.9 Hz, 1H), 7.55 (s, 1H), 7.46 (d, *J* = 8.1 Hz, 2H), 7.44 – 7.34 (m, 3H), 7.30 (d, *J* = 8.5 Hz, 1H), 6.74 (s, 1H), 6.59 (d, *J* = 8.1 Hz, 1H), 4.64 (s, 1H), 4.59 - 4.51 (m, 2H), 4.49 (s, 1H), 4.35 (d, *J* = 15.6 Hz, 1H), 3.88 (d, *J* = 11.1 Hz, 1H), 3.85 (s, 3H), 3.82 - 3.4 (m, 7H), 3.74 – 3.67 (m, 2H), 3.65 – 3.54 (m, 16H), 3.31 (s, 2H), 3.25 (s, 2H), 2.72 (t, *J* = 6.1 Hz, 2H), 2.60 – 2.51 (m, 1H), 2.47 (s, 3H), 2.50 – 2.40 (m, 1H), 2.25 – 2.17 (m, 1H), 2.11 - 2.04 (m, 1H), 1.88 (d, *J* = 13.6 Hz, 6H), 1.03 (s, 9H). HRMS (ESI) calcd for $C_{59}H_{81}ClN_{10}O_{12}PS^+$ $[M+H]^+$, 1219.5177; found, 1219.5181.

(2S,4R)-1-((S)-2-(3-(2-(3-((1-(4-((5-chloro-4-((2-(dimethylphosphoryl)phenyl)amino)pyrimidin-2-yl)amino)-3-methoxyphenyl)piperidin-4-yl)amino)-3-oxopropoxy)ethoxy)propanamido)-3,3-dimethylbutanoyl)-4-hydroxy-N-(4-(4-methylthiazol-5-yl)benzyl)pyrrolidine-2-carboxamide (30). (white solid, 6.1 mg, 28%) ^{1}H NMR (500 MHz, CD_3OD) *δ* 8.93 (s, 1H), 8.30 (dd, *J* = 7.5, 3.5 Hz, 1H), 8.12 (s, 1H), 7.73 – 7.66 (m, 2H), 7.63 – 7.59 (m, 1H), 7.47 – 7.45 (m, 2H), 7.43 – 7.38 (m, 3H), 7.03 (d, *J* = 2.0 Hz, 1H), 6.84 (dd, *J* = 8.8, 2.4 Hz, 1H), 4.66 (s, 1H), 4.60 – 4.54 (m, 1H), 4.51 – 4.47 (m, 2H), 4.39 – 4.34 (m, 1H), 4.03 – 3.96 (m, 1H), 3.91 – 3.87 (m, 1H), 3.92 (s, 3H), 3.80 (dd, *J* = 11.0, 3.8 Hz, 1H), 3.75 – 3.70 (m, 6H), 3.64 – 3.60 (m, 4H), 3.40 – 3.34 (m, 2H), 2.61 – 2.53 (m, 1H), 2.49 – 2.44 (m, 3H), 2.47 (s, 3H), 2.25 – 2.20 (m, 1H), 2.16 – 2.05 (m, 3H), 1.88 (s, 3H), 1.85 (s, 3H), 1.84 – 1.78 (m, 2H), 1.04 (s, 9H). HRMS (ESI) calcd for $C_{54}H_{71}ClN_{10}O_9PS^+$ $[M+H]^+$: 1101.4547, found 1101.4548.

(2S,4R)-1-((S)-2-(tert-butyl)-16-((1-(4-((5-chloro-4-((2-(dimethylphosphoryl)phenyl)amino)pyrimidin-2-yl)amino)-3-methoxyphenyl)piperidin-4-yl)amino)-4,16-dioxo-7,10,13-trioxa-3-azahexadecanoyl)-4-hydroxy-N-(4-(4-methylthiazol-5-yl)benzyl)pyrrolidine-2-carboxamide (31). (white solid, 13.2 mg, 58%) ^{1}H NMR (500 MHz, CD_3OD) *δ* 8.94 (s, 1H), 8.29 (dd, *J* = 7.5, 3.5 Hz, 1H), 8.12 (s, 1H), 7.73 – 7.67 (m, 2H), 7.62 – 7.58 (m, 1H), 7.47 – 7.44 (m, 2H), 7.43 – 7.37 (m,

3H), 7.04 (s, 1H), 6.86 (d, *J* = 8.6 Hz, 1H), 4.65 (s, 1H), 4.59 – 4.50 (m, 2H), 4.50 – 4.47 (m, 1H), 4.38 – 4.33 (m, 1H), 4.03 – 3.97 (m, 1H), 3.92 (s, 3H), 3.89 - 3.86 (m, 1H), 3.80 (dd, *J* = 10.9, 3.9 Hz, 1H), 3.76 – 3.70 (m, 6H), 3.64 – 3.58 (m, 9H), 3.44 – 3.35 (m, 2H), 2.60 – 2.54 (m, 1H), 2.50 – 2.44 (m, 3H), 2.47 (s, 3H), 2.24 – 2.20 (m, 1H), 2.17 – 2.13 (m, 2H), 2.10 – 2.05 (m, 1H), 1.88 (s, 3H), 1.86 – 1.80 (m, 2H), 1.85 (s, 3H), 1.04 (s, 9H). HRMS (ESI) calcd for $C_{56}H_{75}ClN_{10}O_{10}PS^+$ $[M+H]^+$: 1145.4809, found 1145.4807.

N1-(1-(4-((5-chloro-4-((2-(dimethylphosphoryl)phenyl)amino)pyrimidin-2-yl)amino)-3-methoxyphenyl)piperidin-4-yl)-N16-((S)-1-((2S,4R)-4-hydroxy-2-((4-(4-methylthiazol-5-yl)benzyl)carbamoyl)pyrrolidin-1-yl)-3,3-dimethyl-1-oxobutan-2-yl)-4,7,10,13-tetraoxahexadecanediamide (32). (white solid, 13.0 mg, 55%) ^{1}H NMR (500 MHz, CD_3OD) δ 8.99 (s, 1H), 8.25 (dd, *J* = 8.1, 4.0 Hz, 1H), 8.16 (s, 1H), 7.76 (d, *J* = 8.8 Hz, 1H), 7.70 (dd, *J* = 13.9, 7.7 Hz, 1H), 7.63 – 7.59 (m, 1H), 7.48 – 7.46 (m, 2H), 7.44 – 7.41 (m, 3H), 7.15 (d, *J* = 2.3 Hz, 1H), 6.94 (dd, *J* = 8.8, 2.5 Hz, 1H), 4.64 (s, 1H), 4.59 – 4.51 (m, 2H), 4.50 – 4.47 (m, 1H), 4.36 (d, *J* = 15.5 Hz, 1H), 4.08 – 4.01 (m, 1H), 3.93 (s, 3H), 3.90 – 3.87 (m, 1H), 3.79 (dd, *J* = 10.9, 3.7 Hz, 1H), 3.76 – 3.71 (m, 6H), 3.62 – 3.60 (m, 12H), 3.50 (t, *J* = 11.1 Hz, 2H), 2.58 – 2.53 (m, 1H), 2.49 – 2.45 (m, 3H), 2.48 (s, 3H), 2.24 – 2.16 (m, 3H), 2.11 – 2.05 (m, 1H), 1.94 – 1.90 (m, 2H), 1.88 (s, 3H), 1.85 (s, 3H), 1.03 (s, 9H). HRMS (ESI) calcd for $C_{58}H_{79}ClN_{10}O_{11}PS^+$ $[M+H]^+$: 1189.5071, found 1189.5081.

N1-(1-(4-((5-chloro-4-((2-(dimethylphosphoryl)phenyl)amino)pyrimidin-2-yl)amino)-3-methoxyphenyl)piperidin-4-yl)-N19-((S)-1-((2S,4R)-4-hydroxy-2-((4-(4-methylthiazol-5-yl)benzyl)carbamoyl)pyrrolidin-1-yl)-3,3-dimethyl-1-oxobutan-2-yl)-4,7,10,13,16-pentaoxanonadecanediamide (33). (white solid, 19.5 mg, 79%) 1H NMR (500 MHz, CD_3OD) δ 9.05 (s, 1H), 8.23 (dd, *J* = 8.0, 4.1 Hz, 1H), 8.17 (s, 1H), 7.76 (d, *J* = 8.8 Hz, 1H), 7.71 (ddd, *J* = 13.9, 7.8, 1.4 Hz, 1H), 7.64 – 7.59 (m, 1H), 7.50 – 7.46 (m, 2H), 7.44 – 7.40 (m, 3H), 7.19 (d, *J* = 2.4 Hz, 1H), 6.97 (dd, *J* = 8.8, 2.5 Hz, 1H), 4.64 (s, 1H), 4.58 – 4.51 (m, 2H), 4.51 – 4.48 (m, 1H), 4.36 (d, *J* = 15.6 Hz, 1H), 4.09 – 4.03 (m, 1H), 3.94 (s, 3H), 3.90 – 3.87 (m, 1H), 3.80 (dd, *J* = 11.0, 3.9 Hz, 1H), 3.76 – 3.69 (m, 6H), 3.62 – 3.60 (m, 16H), 3.54 (t, *J* = 12.0 Hz, 2H), 2.59 – 2.54 (m, 1H), 2.50 – 2.45 (m, 3H), 2.49 (s, 3H), 2.24 – 2.18 (m, 3H), 2.11 – 2.05 (m, 1H), 1.98 – 1.91 (m, 2H), 1.88 (s, 3H), 1.85 (s, 3H), 1.03 (s, 9H). HRMS (ESI) calcd for $C_{60}H_{83}ClN_{10}O_{12}PS^+$ $[M+H]^+$: 1233.5333, found 1233.5335.

(2S,4R)-1-((S)-2-(3-(2-(3-(4-(1-(4-((5-chloro-4-((2-(dimethylphosphoryl)phenyl)amino)pyrimidin-2-yl)amino)-3-methoxyphenyl)piperidin-4-yl)piperazin-1-yl)-3-oxopropoxy)ethoxy)propanamido)-3,3-dimethylbutanoyl)-4-hydroxy-N-(4-(4-methylthiazol-5-yl)benzyl)pyrrolidine-2-car

boxamide (34). (white solid, 15.4 mg, 50%) ^{1}H NMR (500 MHz, CD_3OD) δ 8.93 (s, 1H), 8.39 (s, 1H), 8.05 (s, 1H), 7.68 (dd, *J* = 14.0, 7.6 Hz, 1H), 7.62 – 7.51 (m, 1H), 7.47 (d, *J* = 8.4 Hz, 2H), 7.45 – 7.36 (m, 3H), 7.29 (d, *J* = 9.4 Hz, 1H), 6.74 (d, *J* = 2.5 Hz, 1H), 6.60 (d, *J* = 7.4 Hz, 1H), 4.66 (s, 1H), 4.60-4.50 (m, 3H), 4.37 (d, *J* = 15.5 Hz, 1H), 3.97 (d, *J* = 13.1 Hz, 2H), 3.89 (d, *J* = 11.2 Hz, 1H), 3.85 (s, 3H), 3.84 – 3.80 (m, 1H), 3.80 – 3.67 (m, 5H), 3.66 – 3.51 (m, 6H), 3.51 – 3.36 (m, 2H), 3.30 (s, 5H), 2.91-2.85 (m, 2H), 2.78 – 2.61 (m, 2H), 2.61 – 2.42 (m, 5H), 2.28-2.21 (m, 3H), 2.11-2.04 (m, 1H), 1.93-1.87 (m, 7H), 1.03 (s, 9H). HRMS (ESI) calcd for $C_{58}H_{78}ClN_{11}O_9PS$ $[M+H]^+$: 1170.5125, found 1170.5127.

(2S,4R)-1-((S)-2-(tert-butyl)-16-(4-(1-(4-((5-chloro-4-((2-(dimethylphosphoryl)phenyl)amino)pyrimidin-2-yl)amino)-3-methoxyphenyl)piperidin-4-yl)piperazin-1-yl)-4,16-dioxo-7,10,13-trioxa-3-azahexadecanoyl)-4-hydroxy-N-(4-(4-methylthiazol-5-yl)benzyl)pyrrolidine-2-carboxamide (35). (white solid, 24.9 mg, 78%) ^{1}H NMR (500 MHz, CD_3OD) δ 8.98 (s, 1H), 8.40 (s, 1H), 8.05 (s, 1H), 7.68 (dd, *J* = 14.0, 7.6 Hz, 1H), 7.62 – 7.52 (m, 1H), 7.51 – 7.46 (m, 2H), 7.45-7.42 (m, 2H), 7.39 (t, *J* = 7.2 Hz, 1H), 7.28 (s, 1H), 6.75 (d, *J* = 2.4 Hz, 1H), 6.61 (d, *J* = 8.7 Hz, 1H), 4.65 (s, 1H), 4.60 – 4.47 (m, 3H), 4.37 (d, *J* = 15.6 Hz, 1H), 3.98 (d, *J* = 12.7 Hz, 2H), 3.89 (d, *J* = 11.2 Hz, 1H), 3.85 (s, 3H), 3.83 – 3.69 (m, 6H), 3.66 – 3.57 (m, 9H), 3.52 – 3.41 (m, 2H), 3.32-3.31 (m, 5H), 2.92-2.86 (m, 2H), 2.65-2.63 (m, 2H), 2.62 – 2.53 (m, 1H), 2.53 – 2.43 (m, 4H), 2.33 – 2.18 (m, 3H), 2.10-2.05 (m, 1H), 1.94-1.87 (m, 8H), 1.03 (s, 9H). HRMS (ESI) calcd for $C_{60}H_{82}ClN_{11}O_{10}PS$ $[M+H]^+$: 1214.5387, found 1214.5377.

(2S,4R)-1-((S)-2-(tert-butyl)-19-(4-(1-(4-((5-chloro-4-((2-(dimethylphosphoryl)phenyl)amino)pyrimidin-2-yl)amino)-3-methoxyphenyl)piperidin-4-yl)piperazin-1-yl)-4,19-dioxo-7,10,13,16-tetraoxa-3-azanonadecanoyl)-4-hydroxy-N-(4-(4-methylthiazol-5-yl)benzyl)pyrrolidine-2-carboxamide (36). (white solid, 23.8 mg, 72%) ^{1}H NMR (500 MHz, CD_3OD) δ 8.94 (d, *J* = 3.1 Hz, 1H), 8.39 (s, 1H), 8.05 (s, 1H), 7.68 (dd, *J* = 13.5, 8.4 Hz, 1H), 7.62 – 7.52 (m, 1H), 7.51 – 7.45 (m, 2H), 7.45-7.41 (m, 2H), 7.38 (t, *J* = 7.8 Hz, 1H), 7.29 (s, 1H), 6.74 (d, *J* = 2.3 Hz, 1H), 6.60 (d, *J* = 8.6 Hz, 1H), 4.65 (s, 1H), 4.59-4.50 (m, 3H), 4.36 (d, *J* = 15.5 Hz, 1H), 3.98 (d, *J* = 12.7 Hz, 2H), 3.92 – 3.83 (m, 4H), 3.82-3.70 (m, 6H), 3.65 – 3.56 (m, 14H), 3.47-3.44 (m, 2H), 3.32 (s, 6H), 2.87 (t, *J* = 12.5 Hz, 2H), 2.67 – 2.54 (m, 2H), 2.51 – 2.43 (m, 4H), 2.32 – 2.18 (m, 3H), 2.10-2.04 (m, 1H), 1.93-1.87 (m, 7H), 1.03 (s, 9H). HRMS (ESI) calcd for $C_{62}H_{86}ClN_{11}O_{11}PS$ $[M+H]^+$: 1258.5650, found 1258.5639.

(2S,4R)-1-((S)-2-(tert-butyl)-22-(4-(1-(4-((5-chloro-4-((2-(dimethylphosphoryl)phenyl)amino

)pyrimidin-2-yl)amino)-3-methoxyphenyl)piperidin-4-yl)piperazin-1-yl)-4,22-dioxo-7,10,13,16,19-pentaoxa-3-azadocosanoyl)-4-hydroxy-N-(4-(4-methylthiazol-5-yl)benzyl)pyrrolidine-2-carboxamide (37). (white solid, 18.7 mg, 55%) ^{1}H NMR (500 MHz, CD_3OD) δ 8.94 (s, 1H), 8.52 – 8.25 (m, 1H), 8.05 (s, 1H), 7.68 (dd, *J* = 14.8, 7.1 Hz, 1H), 7.60-7.55 (m, 1H), 7.51 – 7.46 (m, 2H), 7.45-7.41 (m, 2H), 7.39 (t, *J* = 7.7 Hz, 1H), 7.28 (s, 1H), 6.74 (s, 1H), 6.61 (s, 1H), 4.65 (s, 1H), 4.59 – 4.49 (m, 3H), 4.36 (d, *J* = 15.5 Hz, 1H), 3.98 (d, *J* = 13.0 Hz, 2H), 3.92 – 3.83 (m, 4H), 3.82 – 3.67 (m, 7H), 3.62-3.61 (m, 20H), 3.49-3.44 (m, 2H), 3.34-3.31 (m, 2H), 2.87 (t, *J* = 12.5 Hz, 2H), 2.68 – 2.53 (m, 2H), 2.51 – 2.44 (m, 4H), 2.28-2.20 (m, 3H), 2.10-2.04 (m, 1H), 1.94-1.87 (m, 8H), 1.04 (s, 9H). HRMS (ESI) calcd for $C_{64}H_{90}ClN_{11}O_{12}PS$ $[M+H]^+$: 1302.5912, found 1302.5900.

N1-(1-(4-((5-chloro-4-((2-(dimethylphosphoryl)phenyl)amino)pyrimidin-2-yl)amino)-3-methoxyphenyl)piperidin-4-yl)-N11-((S)-1-((2S,4S)-4-hydroxy-2-((4-(4-methylthiazol-5-yl)benzyl)carbamoyl)pyrrolidin-1-yl)-3,3-dimethyl-1-oxobutan-2-yl)undecanediamide (38, SIAIS117NC) (white solid, 8.2 mg, 28% yield over two steps). ^{1}H NMR (500 MHz, CD_3OD) δ 9.34 (s, 1H), 8.23 (s, 1H), 8.15 (s, 1H), 7.82 – 7.71 (m, 2H), 7.67 (t, J = 7.8 Hz, 1H), 7.50 – 7.45 (m, 6H), 7.18 (d, J = 8.6 Hz, 1H), 4.56 – 4.50 (m, 3H), 4.45 – 4.36 (m, 2H), 4.14-4.10 (m, 1H), 4.04 (dd, J = 10.5, 5.1 Hz, 1H), 3.98 (s, 3H), 3.75-3.68 (m, 6H), 2.53 (s, 3H), 2.50 – 2.40 (m, 1H), 2.34 – 2.20 (m, 8H), 2.13-2.08 (m, 2H), 2.01 – 1.94 (m, 1H), 1.87 (d, J = 13.5 Hz, 6H), 1.62 (d, J = 7.3 Hz, 5H), 1.33 (s, 12H), 1.04 (s, 9H). HRMS (ESI) calcd for $C_{57}H_{77}ClN_{10}O_7PS$ $[M+H]^+$: 1111.5118, found 1111.5111.

Appendix A. Supplementary material

Supplementary material. Details for ^{1}H NMR, ^{13}C NMR spectrum and HPLC analysis of compound 18 (SIAIS117). Experimental methods for biological Materials, cell culture, evaluation of compounds IC50s, western blot, cloning and stable cell line generation, transfection. Brigatinib and all three Brigatinib analogues did not degrade ALK proteins in ALCL-SR cell line. Degradation of ALK proteins in ALCL-SR and NSCLC-H3122 cell lines.

Author information

Corresponding Author

* Email: songxl@shanghaitech.edu.cn

* Email: yangxb@shanghaitech.edu.cn

* Email: Linhf@shanghaitech.edu.cn

* Email: jiangbiao@shanghaitech.edu.cn

Author Contributions

[+]These authors contributed equally to this work.

Notes

The authors declare no competing financial interest.

Acknowledgement

We thank the National Natural Science Foundation of China (Grant Nos. No. 21502114 to B.J. & Grant No. 81602602 to X.S.), Shanghai Natural Science Foundation (Grant No.19ZR1433600 to X.Y.) and China Postdoctoral Science Foundation (2018M632181 to N.S.) and Jing Medicine support.

Reference

[1] B. Hallberg, R.H. Palmer, Mechanistic insight into ALK receptor tyrosine kinase in human cancer biology, Nat Rev Cancer, 13 (2013) 685-700.

[2] J.J. Lin, G.J. Riely, A.T. Shaw, Targeting ALK: Precision Medicine Takes on Drug Resistance, Cancer Discov, 7 (2017) 137-155.

[3] V.R. Holla, Y.Y. Elamin, A.M. Bailey, A.M. Johnson, B.C. Litzenburger, Y.B. Khotskaya, N.S. Sanchez, J. Zeng, M.A. Shufean, K.R. Shaw, J. Mendelsohn, G.B. Mills, F. Meric-Bernstam, G.R. Simon, ALK: a tyrosine kinase target for cancer therapy, Cold Spring Harb Mol Case Stud, 3 (2017) a001115.

[4] C. Zhang, X.R. Han, X. Yang, B. Jiang, J. Liu, Y. Xiong, J. Jin, Proteolysis Targeting Chimeras (PROTACs) of Anaplastic Lymphoma Kinase (ALK), Eur J Med Chem, 151 (2018) 304-314.

[5] D. Das, J. Wang, Y. Li, J. Shi, J. Hong, Design, synthesis of orally bioavailable novel anaplastic lymphoma kinase (ALK) inhibitor diphenylaminopyrimidine analogs and efficacy study on NCI-H2228 xenografts mice model, Bioorg Med Chem Lett, 29 (2019) 1514-1517.

[6] N. Kanaji, S. Bandoh, T. Ishii, A. Tadokoro, N. Watanabe, T. Takahama, R. Haba, O. Imataki, H. Dobashi, T. Matsunaga, Detection of EML4-ALK fusion genes in a few cancer cells from transbronchial cytological specimens utilizing immediate cytology during bronchoscopy, Lung Cancer, 77 (2012) 293-298.

[7] P. Wang, J. Cai, J. Chen, M. Ji, Synthesis and anticancer activities of ceritinib analogs modified in the terminal piperidine ring, Eur J Med Chem, 93 (2015) 1-8.

[8] S. Peters, D.R. Camidge, A.T. Shaw, S. Gadgeel, J.S. Ahn, D.W. Kim, S.I. Ou, M. Perol, R. Dziadziuszko, R. Rosell, A. Zeaiter, E. Mitry, S. Golding, B. Balas, J. Noe, P.N. Morcos, T. Mok, A.T. Investigators, Alectinib versus Crizotinib in Untreated ALK-Positive Non-Small-Cell Lung Cancer, N Engl J Med, 377 (2017) 829-838.

[9] E. Gourd, Alectinib shows CNS efficacy in ALK-positive NSCLC, The Lancet Oncology, 19 (2018).

[10] S. Bedi, S.A. Khan, M.M. AbuKhader, P. Alam, N.A. Siddiqui, A. Husain, A comprehensive review on Brigatinib - A wonder drug for targeted cancer therapy in non-small cell lung cancer, Saudi pharmaceutical journal : SPJ : the official publication of the Saudi Pharmaceutical Society, 26 (2018) 755-763.

[11] D.R. Camidge, H.R. Kim, M.J. Ahn, J.C. Yang, J.Y. Han, J.S. Lee, M.J. Hochmair, J.Y. Li, G.C. Chang, K.H. Lee, C. Gridelli, A. Delmonte, R. Garcia Campelo, D.W. Kim, A. Bearz, F. Griesinger, A. Morabito, E. Felip, R. Califano, S. Ghosh, A. Spira, S.N. Gettinger, M. Tiseo, N. Gupta, J. Haney, D. Kerstein, S. Popat, Brigatinib versus Crizotinib in ALK-Positive Non-Small-Cell Lung Cancer, N Engl J Med, 379 (2018) 2027-2039.

[12] B.J. Solomon, B. Besse, T.M. Bauer, E. Felip, R.A. Soo, D.R. Camidge, R. Chiari, A. Bearz, C.-C. Lin, S.M. Gadgeel, G.J. Riely, E.H. Tan, T. Seto, L.P. James, J.S. Clancy, A. Abbattista, J.-F. Martini, J. Chen, G. Peltz, H. Thurm, S.-H.I. Ou, A.T. Shaw, Lorlatinib in patients with ALK-positive non-small-cell lung cancer: results from a global phase 2 study, The Lancet Oncology, 19 (2018) 1654-1667.

[13] S.N. Waqar, D. Morgensztern, Lorlatinib: a new-generation drug for ALK-positive NSCLC, The Lancet Oncology, 19 (2018) 1555-1557.

[14] S. Yoda, J.J. Lin, M.S. Lawrence, B.J. Burke, L. Friboulet, A. Langenbucher, L. Dardaei, K. Prutisto-Chang, I. Dagogo-Jack, S. Timofeevski, H. Hubbeling, J.F. Gainor, L.A. Ferris, A.K. Riley, K.E. Kattermann, D. Timonina, R.S. Heist, A.J. Iafrate, C.H. Benes, J.K. Lennerz, M. Mino-Kenudson, J.A. Engelman, T.W. Johnson, A.N. Hata, A.T. Shaw, Sequential ALK Inhibitors Can Select for Lorlatinib-Resistant Compound ALK Mutations in ALK-Positive Lung Cancer, Cancer Discov, 8 (2018) 714-729.

[15] A.C. Lai, C.M. Crews, Induced protein degradation: an emerging drug discovery paradigm, Nat Rev Drug Discov, 16 (2017) 101-114.

[16] M. Scheepstra, K.F.W. Hekking, L. van Hijfte, R.H.A. Folmer, Bivalent Ligands for Protein Degradation in Drug Discovery, Comput Struct Biotechnol J, 17 (2019) 160-176.

[17] L.H. Jones, Small-Molecule Kinase Downregulators, Cell Chem Biol, 25 (2018) 30-35.

[18] B. Jiang, E.S. Wang, K.A. Donovan, Y. Liang, E.S. Fischer, T. Zhang, N.S. Gray, Development of Dual and Selective Degraders of Cyclin-Dependent Kinases 4 and 6, Angew Chem Int Ed Engl, 58 (2019) 6321-6326.

[19] C.H. Kang, D.H. Lee, C.O. Lee, J. Du Ha, C.H. Park, J.Y. Hwang, Induced protein degradation of anaplastic lymphoma kinase (ALK) by proteolysis targeting chimera (PROTAC), Biochem Biophys Res Commun, 505 (2018) 542-547.

[20] A.D. Buhimschi, H.A. Armstrong, M. Toure, S. Jaime-Figueroa, T.L. Chen, A.M. Lehman, J.A. Woyach, A.J. Johnson, J.C. Byrd, C.M. Crews, Targeting the C481S Ibrutinib-Resistance Mutation in Bruton's Tyrosine Kinase Using PROTAC-Mediated Degradation, Biochemistry-Us, 57 (2018) 3564-3575.

[21] M.M. Savitski, N. Zinn, M. Faelth-Savitski, D. Poeckel, S. Gade, I. Becher, M. Muelbaier, A.J. Wagner, K. Strohmer, T. Werner, S. Melchert, M. Petretich, A. Rutkowska, J. Vappiani, H. Franken, M. Steidel, G.M. Sweetman, O. Gilan, E.Y.N. Lam, M.A. Dawson, R.K. Prinjha, P. Grandi, G. Bergamini, M. Bantscheff, Multiplexed Proteome Dynamics Profiling Reveals Mechanisms Controlling Protein Homeostasis, Cell, 173 (2018) 260-274 e225.

[22] A. Pawar, P.N. Gollavilli, S. Wang, I.A. Asangani, Resistance to BET Inhibitor Leads to Alternative Therapeutic Vulnerabilities in Castration-Resistant Prostate Cancer, Cell Rep, 22 (2018) 2236-2245.

[23] S. Piya, H. Mu, S. Bhattacharya, P.L. Lorenzi, R.E. Davis, T. McQueen, V. Ruvolo, N. Baran, Z. Wang, Y. Qian, C.M. Crews, M. Konopleva, J. Ishizawa, M.J. You, H. Kantarjian, M. Andreeff, G. Borthakur, BETP degradation simultaneously targets acute myelogenous leukemia stem cells and the microenvironment, J Clin Invest, 130 (2019).

[24] C.E. Powell, Y. Gao, L. Tan, K.A. Donovan, R.P. Nowak, A. Loehr, M. Bahcall, E.S. Fischer, P.A. Janne, R.E. George, N.S. Gray, Chemically Induced Degradation of Anaplastic Lymphoma Kinase (ALK), J Med Chem, 61 (2018) 4249-4255.

[25] B.Z. Stanton, E.J. Chory, G.R. Crabtree, Chemically induced proximity in biology and medicine, Science, 359 (2018).

[26] X. Han, C. Wang, C. Qin, W. Xiang, E. Fernandez-Salas, C.Y. Yang, M. Wang, L. Zhao, T. Xu, K. Chinnaswamy, J. Delproposto, J. Stuckey, S. Wang, Discovery of ARD-69 as a Highly Potent Proteolysis Targeting Chimera (PROTAC) Degrader of Androgen Receptor (AR) for the Treatment of Prostate Cancer, J Med Chem, 62 (2019) 941-964.

[27] J. Hu, B. Hu, M. Wang, F. Xu, B. Miao, C.Y. Yang, M. Wang, Z. Liu, D.F. Hayes, K. Chinnaswamy, J. Delproposto, J. Stuckey, S. Wang, Discovery of ERD-308 as a Highly Potent Proteolysis Targeting Chimera (PROTAC) Degrader of Estrogen Receptor (ER), J Med Chem, 62 (2019) 1420-1442.

[28] J.S. Schneekloth, Jr., F.N. Fonseca, M. Koldobskiy, A. Mandal, R. Deshaies, K. Sakamoto, C.M. Crews, Chemical genetic control of protein levels: selective in vivo targeted degradation, J Am Chem Soc, 126 (2004) 3748-3754.

[29] Q. Zhao, T. Lan, S. Su, Y. Rao, Induction of apoptosis in MDA-MB-231 breast cancer cells by a PARP1-targeting PROTAC small molecule, Chem Commun (Camb), 55 (2019) 369-372.

[30] G.M. Burslem, J. Song, X. Chen, J. Hines, C.M. Crews, Enhancing Antiproliferative Activity and Selectivity of a FLT-3 Inhibitor by Proteolysis Targeting Chimera Conversion, J Am Chem Soc, 140 (2018) 16428-16432.

[31] Q. Zhao, C. Ren, L. Liu, J. Chen, Y. Shao, N. Sun, R. Sun, Y. Kong, X. Ding, X. Zhang, Y. Xu, B. Yang, Q. Yin, X. Yang, B. Jiang, Discovery of SIAIS178 as an Effective BCR-ABL Degrader by Recruiting Von Hippel-Lindau (VHL) E3 Ubiquitin Ligase, J Med Chem, 62 (2019) 9281-9298.

[32] X. Qiu, N. Sun, Y. Kong, Y. Li, X.B. Yang, B. Jiang, Chemoselective Synthesis of Lenalidomide-Based PROTAC Library Using Alkylation Reaction, Org Lett, 21 (2019) 3838-3841.

[33] S. Zhang, R. Anjum, R. Squillace, S. Nadworny, T. Zhou, J. Keats, Y.Y. Ning, S.D. Wardwell, D. Miller, Y. Song, L. Eichinger, L. Moran, W.S. Huang, S.Y. Liu, D. Zou, Y. Wang, Q. Mohemmad, H.G. Jang, E. Ye, N. Narasimhan, F. Wang, J. Miret, X.T. Zhu, T. Clackson, D. Dalgarno, W.C. Shakespeare, V.M. Rivera, The Potent ALK Inhibitor Brigatinib (AP26113) Overcomes Mechanisms of Resistance to First- and Second-Generation ALK Inhibitors in Preclinical Models, Clin Cancer Res, 22 (2016) 5527-5538.

[34] D.R. Camidge, D.W. Kim, M. Tiseo, C.J. Langer, M.J. Ahn, A.T. Shaw, R.M. Huber, M.J. Hochmair, D.H. Lee, L.A. Bazhenova, K.A. Gold, S.I. Ou, H.L. West, W. Reichmann, J. Haney, T. Clackson, D. Kerstein, S.N. Gettinger, Exploratory Analysis of Brigatinib Activity in Patients With Anaplastic Lymphoma Kinase-Positive Non-Small-Cell Lung Cancer and Brain Metastases in Two Clinical Trials, J Clin Oncol, 36 (2018) 2693-2701.

[35] J. Wu, J. Savooji, D. Liu, Second- and third-generation ALK inhibitors for non-small cell lung cancer, J Hematol Oncol, 9 (2016) 19.

[36] J.K. Sabari, F.C. Santini, A.M. Schram, I. Bergagnini, R. Chen, C. Mrad, W.V. Lai, K.C. Arbour, A. Drilon, The activity, safety, and evolving role of brigatinib in patients with ALK-rearranged non-small cell lung cancers, Onco Targets Ther, 10 (2017) 1983-1992.

[37] W.S. Huang, S. Liu, D. Zou, M. Thomas, Y. Wang, T. Zhou, J. Romero, A. Kohlmann, F. Li, J. Qi, L. Cai, T.A. Dwight, Y. Xu, R. Xu, R. Dodd, A. Toms, L. Parillon, X. Lu, R. Anjum, S. Zhang, F. Wang, J. Keats, S.D. Wardwell, Y. Ning, Q. Xu, L.E. Moran, Q.K. Mohemmad, H.G. Jang, T. Clackson, N.I. Narasimhan, V.M. Rivera, X. Zhu, D. Dalgarno, W.C. Shakespeare, Discovery of Brigatinib (AP26113), a Phosphine Oxide-Containing, Potent, Orally Active Inhibitor of Anaplastic Lymphoma Kinase, J Med Chem, 59 (2016) 4948-4964.

[38] D.W. Kim, M. Tiseo, M.J. Ahn, K.L. Reckamp, K.H. Hansen, S.W. Kim, R.M. Huber, H.L. West, H.J.M. Groen, M.J. Hochmair, N.B. Leighl, S.N. Gettinger, C.J. Langer, L.G. Paz-Ares Rodriguez, E.F. Smit, E.S. Kim, W. Reichmann, F.G. Haluska, D. Kerstein, D.R. Camidge, Brigatinib in Patients With Crizotinib-Refractory Anaplastic Lymphoma Kinase-Positive Non-Small-Cell Lung Cancer: A Randomized, Multicenter Phase II Trial, J Clin Oncol, 35 (2017) 2490-2498.

[39] S. Zhang, R. Anjum, R. Squillace, S. Nadworny, T. Zhou, J. Keats, Y. Ning, S.D. Wardwell, D. Miller, Y. Song, L. Eichinger, L. Moran, W.S. Huang, S. Liu, D. Zou, Y. Wang, Q. Mohemmad, H.G. Jang, E. Ye, N. Narasimhan, F. Wang, J. Miret, X. Zhu, T. Clackson, D. Dalgarno, W.C. Shakespeare, V.M. Rivera, The Potent ALK Inhibitor Brigatinib (AP26113) Overcomes Mechanisms of Resistance to First- and Second-Generation ALK Inhibitors in Preclinical Models, Clin Cancer Res, 22 (2016) 5527-5538.

[40] N. Takegawa, H. Hayashi, N. Iizuka, T. Takahama, H. Ueda, K. Tanaka, M. Takeda, K. Nakagawa, Transformation of ALK rearrangement-positive adenocarcinoma to small-cell lung cancer in association with acquired resistance to alectinib, Ann Oncol, 27 (2016) 953-955.

[41] S. Fujita, K. Masago, N. Katakami, Y. Yatabe, Transformation to SCLC after Treatment with the ALK Inhibitor Alectinib, J Thorac Oncol, 11 (2016) e67-72.

[42] Y.J. Cha, B.C. Cho, H.R. Kim, H.J. Lee, H.S. Shim, A Case of ALK-Rearranged Adenocarcinoma with Small Cell Carcinoma-Like Transformation and Resistance to Crizotinib, J Thorac Oncol, 11 (2016) e55-e58.

[43] S. Miyamoto, S. Ikushima, R. Ono, N. Awano, K. Kondo, Y. Furuhata, K. Fukumoto, T. Kumasaka, Transformation to small-cell lung cancer as a mechanism of acquired resistance to crizotinib and alectinib, Jpn J Clin Oncol, 46 (2016) 170-173.

Graphical Abstract

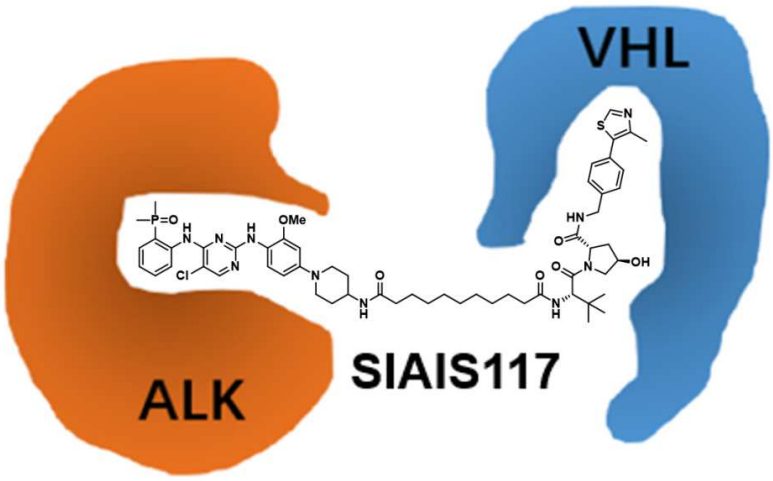

IC_{50} = 1.7± 1.0 nM in ALCL-SR cell line, DC_{50} = 7.0 nM in SR cell line

DC_{50} = 51.0 nM in NSCLC-H2228 cell line

DC_{50} = 189 nM in ALK-G1202R mutant cell line

Highlight

Degraders based on Brigatinib-PROTAC has been designed and identified firstly.

SIAIS117 could degrade ALK G1202R point mutation effectively.

SIAIS117 shows durative degradation property.

Declaration of interests

☒ The authors declare that they have no known competing financial interests or personal relationships that could have appeared to influence the work reported in this paper.

☐The authors declare the following financial interests/personal relationships which may be considered as potential competing interests: